

In presenting this dissertation as a partial fulfillment of the requirements for an advanced degree from the Georgia Institute of Technology, I agree that the Library of the Institution shall make it available for inspection and circulation in accordance with its regulations governing materials of this type.

I agree that permission to copy from or to publish from, this dissertation may be granted by the professor under whose direction it was written, or, in his absence, by the Dean of the Graduate Division when such copying or publication is solely for scholarly purposes and does not involve financial gain.

It is understood that any copying from, or publication of, this dissertation which involves potential financial gain will not be allowed without written permission.

~~Robby Eugène Cox~~

THE EFFECT OF ASPHALT CONTENT AND TEMPERATURE,  
ON THE TRIAXIAL PROPERTIES OF AN  
ASPHALT CONCRETE MIX

A THESIS

Presented to

the Faculty of the Graduate Division

by

Bobby Eugene Cox

In Partial Fulfillment

of the Requirements for the Degree

Master of Science in Civil Engineering

Georgia Institute of Technology

August, 1960

26  
12R-A

THE EFFECT OF ASPHALT CONTENT AND TEMPERATURE  
ON THE TRIAXIAL PROPERTIES OF AN  
ASPHALT CONCRETE MIX

Approved:

*R. J. Paquette*  
Radnor J. Paquette  
Thesis Advisor

*A. B. Vesic*  
Aleksandar B. Vesic  
Thesis Advisor

*D. O. Covalt*  
Donald O. Covalt  
Member of Reading Committee

Date Approved by Chairmen August 5 '60

BOUND BY THE NATIONAL LIBRARY BINDERY CO. OF GA.

## ACKNOWLEDGEMENTS

Grateful appreciation is extended to Dr. A. Vesic and Professor Radnor J. Paquette for their encouragement, stimulating thoughts and advice while serving as advisors for this research. The author also wishes to express his gratitude for Dr. D. O. Covalt's helpful criticisms and suggestions while serving as a member of the reading committee.

The Georgia Highway Department is to be thanked for the use of their kneading compaction machine while molding the necessary test specimens. Gratitude is extended to the Georgia Highway Laboratory Staff for their patience during this trying period of research.

Acknowledgement is also made to the Shell Foundation for granting a fellowship and thus making this year of graduate study possible.

## TABLE OF CONTENTS

	Page
ACKNOWLEDGEMENTS .....	iii
LIST OF TABLES .....	v
LIST OF ILLUSTRATIONS.....	vi
ABSTRACT .....	ix
CHAPTER	
I. INTRODUCTION.....	1
The Triaxial Test	
Mohr's Circle	
Triaxial Compression Test Specimen	
II. EQUIPMENT AND MATERIALS .....	10
III. PROCEDURE .....	14
Aggregate Preparation	
Compaction	
Bulk Specific Gravity	
Preparation for Triaxial Testing	
Triaxial Testing	
Computation of Triaxial Strength Properties	
IV. RESULTS .....	20
Compaction and Asphalt Content	
Angle of Internal Friction and Asphalt Content	
Shear Strength and Asphalt Content	
Angle of Internal Friction and Temperature	
Shear Strength and Temperature	
Stress and Deformation	
V. CONCLUSIONS AND RECOMMENDATIONS .....	33
APPENDICES .....	35
BIBLIOGRAPHY .....	56

## LIST OF TABLES

Table	Page
1. Schedule of Compaction Blows for 4-Inch Diameter Specimen .....	16
2. Bulk Specific Gravity Factors for Various Asphalt Contents .....	18

## LIST OF ILLUSTRATIONS

Figure	Page
1. Schematic Diagram of Triaxial Compression Testing Device .....	4
2. The Mohr Diagram and Stress Circle .....	4
3. The Mohr Rupture Diagram .....	5
4. Aggregate Gradation Curve .....	11
5. Specimen Compaction Apparatus .....	13
6. Triaxial Test Apparatus .....	13
7. Per cent Voids vs. Asphalt Content Curves .....	21
8. Bulk Specific Gravity vs. Asphalt Content .....	21
9. Angle of Internal Friction vs. Asphalt Content From Tests at 140° F .....	23
10. The Effect of Compaction on the Angle of Internal Friction of Specimens Tested at 140° F .	23
11. Unconfined Shear Strength and Apparent Cohesion vs. Asphalt Content Curves at 140° F .....	24
12. The Effect of Temperature on the Angle of Internal Friction of Specimens Containing 6 per cent Asphalt .....	28
13. The Effect of Test Temperature on Unconfined Shear Strength and Apparent Cohesion of Specimens Containing 6 per cent Asphalt .....	28
14. Axial Stress vs. Asphalt Content for Lateral Pressures of 10, 20, and 40 psi at 0.5, 1.0, and 1.5 per cent Strain. Test Temperature is 140° F .....	32
15. Differential Stress vs. Strain Curves for Specimens Containing 4.0 per cent Asphalt at 140° F .....	40

## List of Illustrations (Cont.)

Figure	Page
16. Differential Stress vs. Strain Curves for Specimens Containing 5.0 per cent Asphalt at 140° F .....	41
17. Differential Stress vs. Strain Curves for Specimens Containing 6.0 per cent Asphalt at 140° F .....	42
18. Differential Stress vs. Strain Curves for Specimens Containing 7.0 per cent Asphalt at 140° F .....	43
19. Differential Stress vs. Strain Curves for Specimens Containing 8.0 per cent Asphalt at 140° F .....	44
20. Differential Stress vs. Strain Curves for Specimens Containing 6.0 per cent Asphalt at 70° F .....	45
21. Differential Stress vs. Strain Curves for Specimens Containing 6.0 per cent Asphalt at 35° F .....	46
22. Differential Stress vs. Strain Curves for Specimens Containing 6.0 per cent Asphalt at 0° F .....	47
23. Axial Stress at Rupture vs. Lateral Pressure for Specimens Containing 4.0 per cent Asphalt at 140° F .....	51
24. Axial Stress at Rupture vs. Lateral Pressure for Specimens Containing 5.0 per cent Asphalt at 140° F .....	51
25. Axial Stress at Rupture vs. Lateral Pressure for Specimens Containing 6.0 per cent Asphalt at 140° F .....	52
26. Axial Stress at Rupture vs. Lateral Pressure for Specimens Containing 7.0 per cent Asphalt at 140° F .....	52
27. Axial Stress at Rupture vs. Lateral Pressure for Specimens Containing 8.0 per cent Asphalt at 140° F .....	53

## List of Illustrations (Cont.)

Figure	Page
28. The Effect of Temperature on Axial Rupture Stress of Specimens Tested at Lateral Pressures of 10, 20, and 40 psi .....	54
29. Axial Stress at Rupture vs. Lateral Pressure for Specimens Containing 6.0 per cent Asphalt at Test Temperatures of 0, 10, 20, 40, 60, 80, 100, 120, and 140° F .....	55

## ABSTRACT

THE EFFECT OF ASPHALT CONTENT AND TEMPERATURE  
ON THE TRIAXIAL PROPERTIES OF AN  
ASPHALT CONCRETE MIX

Bobby Eugene Cox

57 pages

Directed by

Radnor J. Paquette and Aleksandar B. Vesic

This research was undertaken to determine the effect of asphalt content and temperature on the load carrying ability of an asphaltic concrete pavement if it was molded by a constant "kneading" compaction effort and loads were applied at a constant rate. The method of analysis chosen was the open triaxial test with application of test results to the Mohr theory of stress and rupture for straight rupture lines.

The five asphalt contents chosen were equally spaced through the entire possible range of values. For each asphalt content chosen, sufficient 4-inch diameter by 8-inch cylindrical specimens were compacted by 250 blows at 335 psi foot pressure of a kneading compaction machine to allow two specimens to be loaded at a constant rate of 0.05 inches per minute in an "open type" triaxial cell at each of three lateral pressures (10, 20, and 40 psi). The temperature chosen for these tests was 140° F and the effect of temperature

on the strength properties of this mix at one asphalt content was studied by repeating the above procedure at test temperatures of 70, 35, and 0° F.

Voids characteristics were computed from densities obtained by the wax coating method. This data along with the triaxial properties of angle of internal friction, cohesion, and unconfined shear strength are presented on charts and graphs in the text. Also stress vs. strain curves are presented for each specimen loaded.

This pavement exhibits an angle of internal friction that varies inversely with the per cent voids existing in the mineral aggregate. It has an unconfined shear strength that appears to reduce directly with the volume of asphalt added to the mix up to the point of maximum compaction, if the angle of internal friction did not vary. Results indicate that this rate of strain is sufficiently slow to prevent viscous shear of the binder from influencing the values of angle of internal friction of this asphalt mix for test temperature above about 120° F. As specimens were tested at lower temperatures this mix exhibits a decreasing angle of internal friction between 100 and 60° F and increasing values between 60° F and 10° F. Unconfined shear strength increased with decreasing temperatures due to increased binder viscosity.

## CHAPTER I

## INTRODUCTION

General--Prior to 1945, practically all asphalt pavement design procedures had an empirical basis. This was necessary to solve the problem at hand, but it was an expedient since these procedures afforded no physical picture of the material's inner working mechanism. A completely rational asphalt pavement design method cannot be developed until the material's physical structure is better understood. A complete solution to the asphalt pavement's mechanism has not yet been devised, even though considerable effort has been exerted by asphalt paving technologists and rheological scientists.

The Triaxial Test.--The most promising approach to appraising the load carrying characteristics of granular materials is the triaxial compression test. Data from triaxial test supplies information concerning the vertical load required to produce deformation and failure of a material under different conditions of lateral support. This lateral support corresponds to the support afforded the material under a loaded area by the surrounding material. The principle of triaxial compression test is illustrated by Figure 1. This schematic diagram shows a cylindrical specimen encased in

two metal disks and a rubber membrane. The porous stone in the base serves as a drainage outlet for any fluid inside the sample and thereby insures atmospheric pressure inside the specimen with the rubber membrane preventing the cell fluid's entrance into the sample. Pressure is applied from a constant air supply and recorded on the pressure gage. This pressure is transmitted hydrostatically to the specimen's sides and top by the cell fluid, and thus the specimen is given lateral support ( $\sigma_3$ ) equal to the pressure gage reading in units of force per unit area. Also a vertical pressure, equal to the lateral pressure, is distributed over the specimen's top, which in effect applies a force per unit area by dividing  $P$  by the specimen's circular area, and the two are added to obtain the total axial stress.

The specimen is deformed at a constant rate of deformation until it fails by sliding along an inclined surface similar to  $aa$  or  $bb$  on Figure 1. The triaxial compression test informs us of the intensity of vertical pressure,  $\sigma_1$ , in force per unit area that is required to produce failure of the specimen at a given horizontal pressure,  $\sigma_3$ . Since the failure occurs along an inclined surface of sliding, the state of stress along this surface is of interest.

Mohr Circle.--When the stress acting on a plane consists of only a component acting normal to the plane, this normal stress is termed a principal stress.  $\sigma_1$  and  $\sigma_3$  are principal stresses by the nature of their application. No shear can

exist along the test specimen's vertical sides since the pressure is hydrostatically applied and the ball connection at the specimen's top prevents shear in that plane. Then the data from triaxial test is applicable to a shear stress vs. normal stress diagram known as the Mohr Diagram, Figure 2. According to Mohr (1), a circle drawn through the ordinates,  $\sigma_1$ , and  $\sigma_3 = \sigma_2$ , represents the state of normal and shear stress in any plane of a material loaded by  $\sigma_1$  and,  $\sigma_3 = \sigma_2$ . Since  $\sigma_3$  equals  $\sigma_2$  only a two-dimensional diagram will be used here. For example, the stress components along plane aa may be represented by the coordinates to point x,  $(\sigma_n, \tau)$ . By the same token stress components along any plane through the specimen may be determined from the circle by simply knowing the angle  $\alpha$ .

Mohr Theory of Rupture.--An important approach to studying the properties of a particular material with triaxial compression tests is the evaluation of stress conditions at rupture. A theory of stress conditions in a material at rupture, contributed by Otto Mohr, has been found to apply particularly well to soils, asphalt pavement, concrete, and stone. "Mohr reasoned that yield or failure within a material was not caused by normal stresses alone reaching a certain maximum or yield point or by shear stresses alone reaching a maximum, but by critical combinations of both shear and normal stresses. The failure is essentially by shear, but the critical shear stress is governed by the normal stress acting on the potential surface of failure" (2).

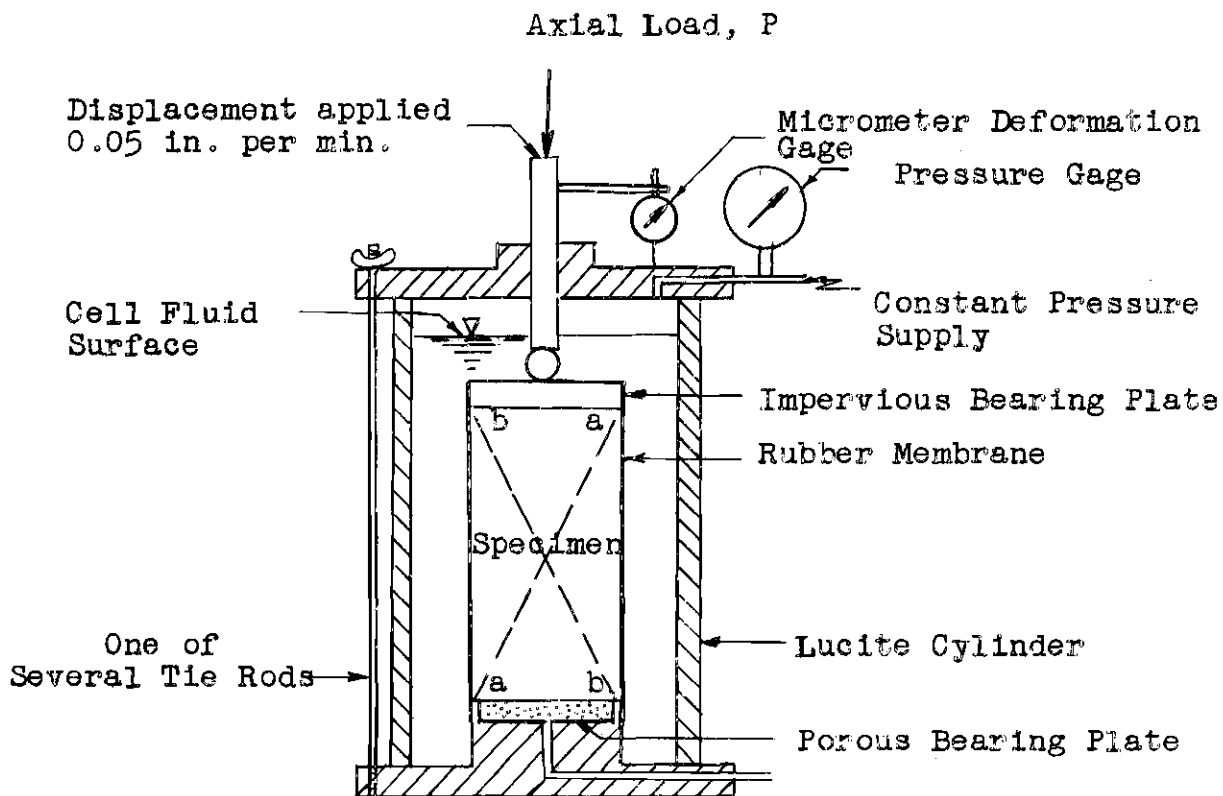


Figure 1. Schematic Diagram of Triaxial Compression Testing Device.

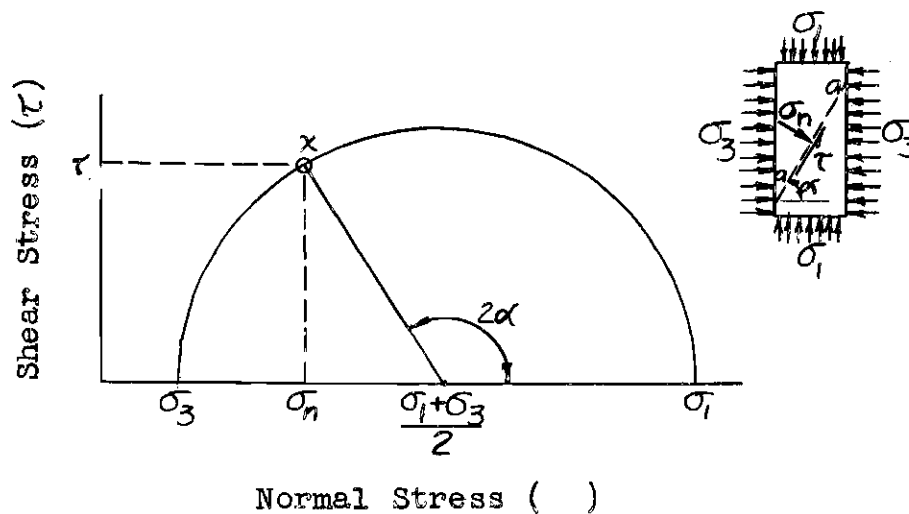


Figure 2. The Mohr Diagram and Stress Circle.

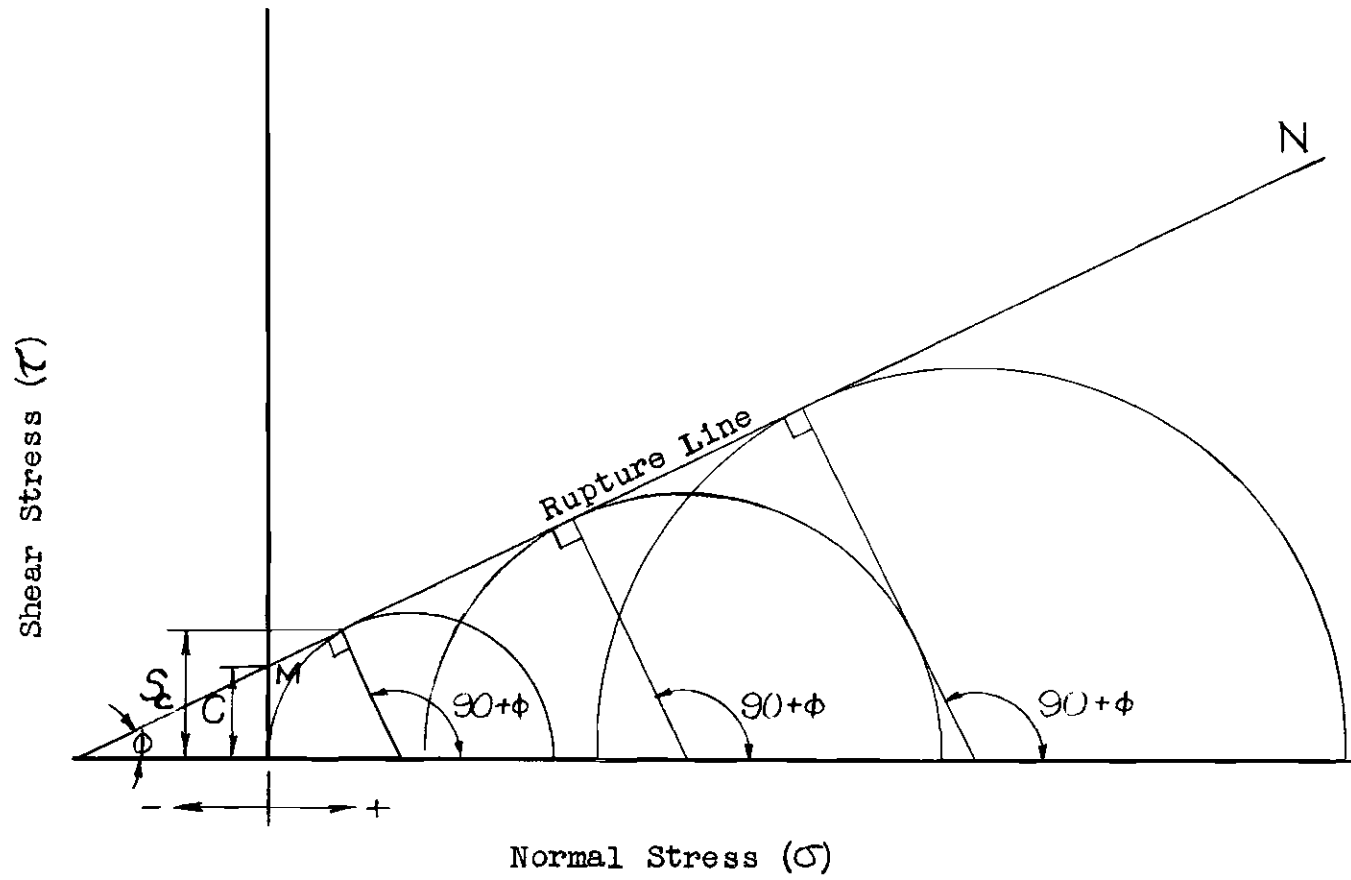


Figure 3. Mohr Rupture Diagram.

Triaxial Compression Test results containing rupture principal stress values,  $\sigma_1$  and  $\sigma_3$ , for a series of samples tested at various lateral pressures substantiates Mohr's Rupture Theory. Figure 3 shows a series of such test results plotted on a Mohr diagram. The line drawn tangent to all these circles, known as Mohr's envelope of rupture, represents the critical combination of shear and normal stresses necessary to induce rupture in the test specimens. This is an accepted method for analysis of triaxial test data, and the material's strength properties are usually reported in terms of  $\phi$ , the slope of a straight Mohr rupture envelope, and  $C$ , the shear intercept at zero normal stress. The term apparent cohesion,  $C$ , stems from a mathematical representation of this line known as Coulomb's equation.

The Triaxial Compression Test Specimen.--Triaxial testing procedures have undergone considerable scrutiny during the past twelve years by such interested parties as members of the Triaxial Institute, and certain specifications have been set up for a rational triaxial specimen. Prior to 1947, there was much controversy over the specimen's dimensions, loading rate, and particularly the compaction method used in molding asphaltic concrete specimen for triaxial testing.

Practically all authorities on the subject agree that the specimen shall have a diameter at least four times that of its largest particle and shall possess a height to diameter ratio of at least two, and a compacted asphalt pavement

specimen shall meet aggregate orientation and density requirements similar to those obtained from field cores.

The compaction method used on laboratory specimens is of prime importance since these specimens should have mechanical properties that correlate with those in the field. A "kneading" type compaction method has been developed that produces specimens whose aggregate structure is very similar to field cores (3). The most important improvement over the conventional drop hammer or static compaction methods was realized in asphaltic mixes containing coarse fractions of aggregate. Lack of particle movement freedom prevented the larger particles from seeking a more favorable orientation to attain the desired density, while the compaction equipment used in construction allowed this movement. Consequently, the particle points under static compaction had a tendency to crush into each other and puncture the asphalt film. Several investigations (4) have been conducted to compare test results of samples molded with the static, drop hammer, and kneading compaction methods. Results of these tests prompted the following statement in the minutes of the May, 1948, meeting of American Society for Testing Materials Committee D-4 on Road and Paving Materials. "The committee unanimously agreed that kneading compaction methods were necessary to useful investigation; otherwise, there could be no certainty that the samples tested in the laboratory would correlate in mechanical properties with those placed

in the field" (5). The Hveem machine uses a cam shaped foot to apply a load for 0.36 seconds dwell time. The foot for a 4-inch diameter specimen has an area of only 3.2 square inches; hence, several blows on the rotating specimen are required for a "coverage." With sufficient foot pressure and number of blows, asphaltic mixture, fed in uniformly as the machine operates, may be compacted to uniformly high densities.

Messrs. Monismith and Vallerga published a paper (6) in the 1952 Journal of Association of Asphalt Paving Technologists concerning the effect of pavement density on the triaxial stability of samples molded with a kneading compactor. A series of curves was presented which showed an increase in mix density with increase in asphalt content and also with an increase in compactive effort employed. It also indicated that the increase in compactive effort resulted in a corresponding increase in mix stability at the lower asphalt contents, and at the higher asphalt contents, especially after the point of maximum mix density had been reached, the mix stability decreased to approximately the same low value. Results shown here also indicate that the most thoroughly compacted mix showed the greatest loss in stability.

This research is essentially an extension of Messrs. Monismith and Vallerga's paper. Using the same asphalt grade; an identical aggregate gradation, but a less dense

Georgia granite; and the same molding and test temperatures; six specimens at each asphalt content were compacted at one of the intermediate compactive efforts, 250 blows at 335 psi foot pressure. For each asphalt content, two specimens were loaded triaxially with the same loading rate (0.05 inches per minute), at each of three lateral pressures (10, 20, and 40 psi). Then an asphalt content was selected which would probably make a good pavement, and the above procedure was repeated at test temperatures of 70, 35 and 0° F. The objective of these tests was to show the effect of asphalt content and temperature on the load-carrying ability of a pavement with a constant compaction effort and loading rate.

## CHAPTER II

## EQUIPMENT AND MATERIALS

Materials.--A crushed granite from Consolidated Quarries, Inc. near Lithonia, Georgia, was used for sizes coarser than the No. 200 sieve. Aggregate finer than the No. 200 sieve was marble aggregate filler from Marble Products Company of Georgia at Whitestone, Georgia. The aggregate gradation, shown in Figure 4, conforms to requirements (7) of the Georgia Highway Department for a "type D" asphaltic concrete pavement. The respective bulk specific gravities of the marble and granite was 2.80 and 2.61. The granite shows a wear of less than 60 per cent when subjected to the Los Angeles Abrasion test (AASHO T-96) and has been used extensively in Georgia Highway pavements. The binder was a paving grade of asphalt cement (AC-8) with a penetration of 85 to 100 at 77° F, and a specific gravity of 1.012 at 77° F.

Equipment.--The mixing equipment included mixing spoons, bowls, and storage pans. The mix was batched to the nearest 1.0 gram with the use of Toledo Scales. The electro-hydraulic kneading compactor (No. 1 in Figure 5) was built by Soil Test, Inc. of Chicago, Illinois, to compact samples that meet specifications for the Hveem asphaltic concrete design method (8). The material was fed into the 4-inch diameter split mold

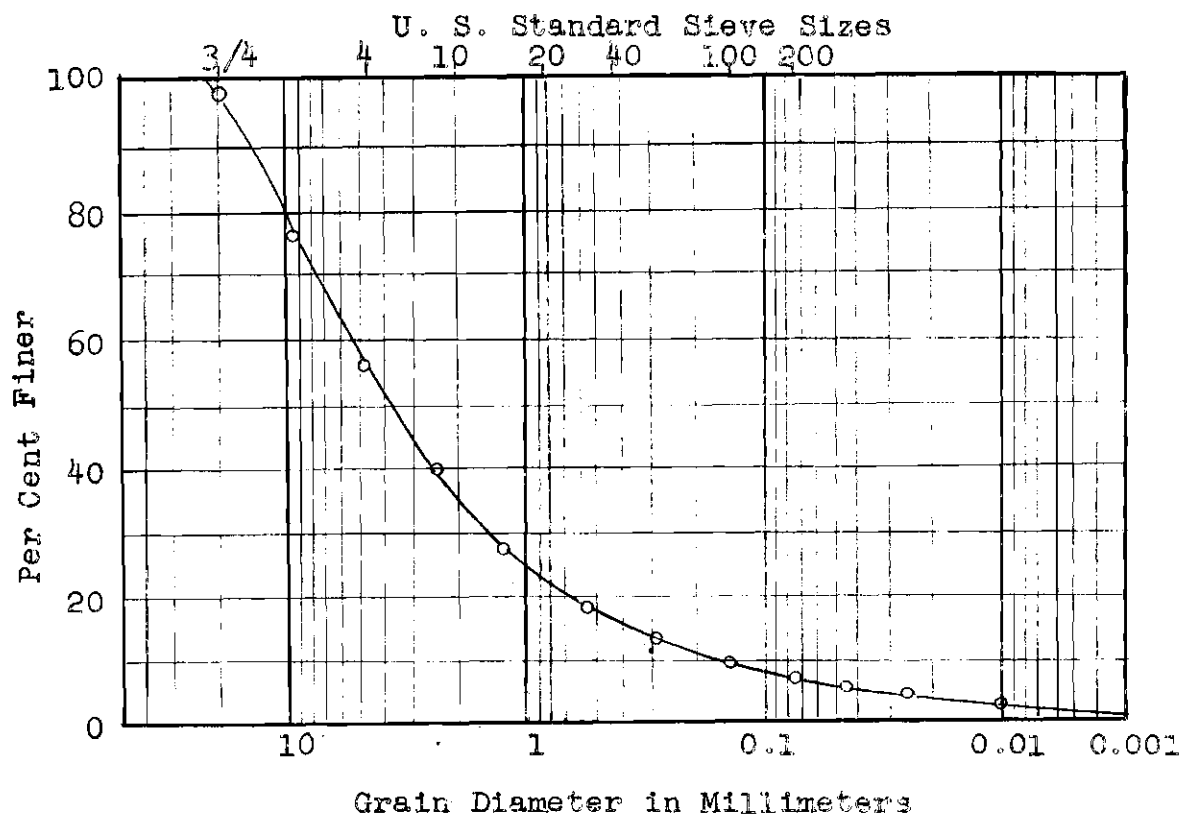


Figure 4. Aggregate Gradation Curve.

(No. 2 in Figure 5) from eight 1-inch by 2-inch by 12-inch aluminum sleeves (No. 3 in Figure 5) and the mold was secured to the compactor turntable with a mold holder (No. 4 in Figure 5).

The triaxial cell (No. 1 in Figure 6), designed and built by the School of Civil Engineering personnel of Georgia Institute of Technology, has a 12-inch diameter chamber and a depth of 18 inches. This allows the sample to be surrounded by a 4 inch thick jacket of constant temperature fluid. The lateral support pressure was indicated by pressure gage readings on the cell with accuracy of  $\pm 0.5$  pounds per square inch and this pressure was applied from a regulated air source. A Tinius-Olsen loading machine applied the load at a constant deformation rate of 0.05 inches per minute to a 20,000 pound capacity. Samples tested at a temperature of  $0^{\circ}$  F were loaded with a 200,000 pound capacity Riehle loading machine at the same deformation rate. Data from both machines was recorded to 2 per cent accuracy and deformation was recorded from a micrometer dial gage to  $\pm 0.001$  inch.

A freezer, equipped with a temperature selection dial and sufficient thermostatic controls to maintain any desired temperature between  $+ 75$  and  $-25^{\circ}$  F to  $\pm 2^{\circ}$  F accuracy, was used to maintain the test temperature of the cell fluid and specimens at test temperatures of 0, 35, and  $70^{\circ}$  F. An electric oven was used to maintain the temperature of mixing, compaction, and the  $140^{\circ}$  F test specimens to accuracy of  $\pm 2^{\circ}$  F.

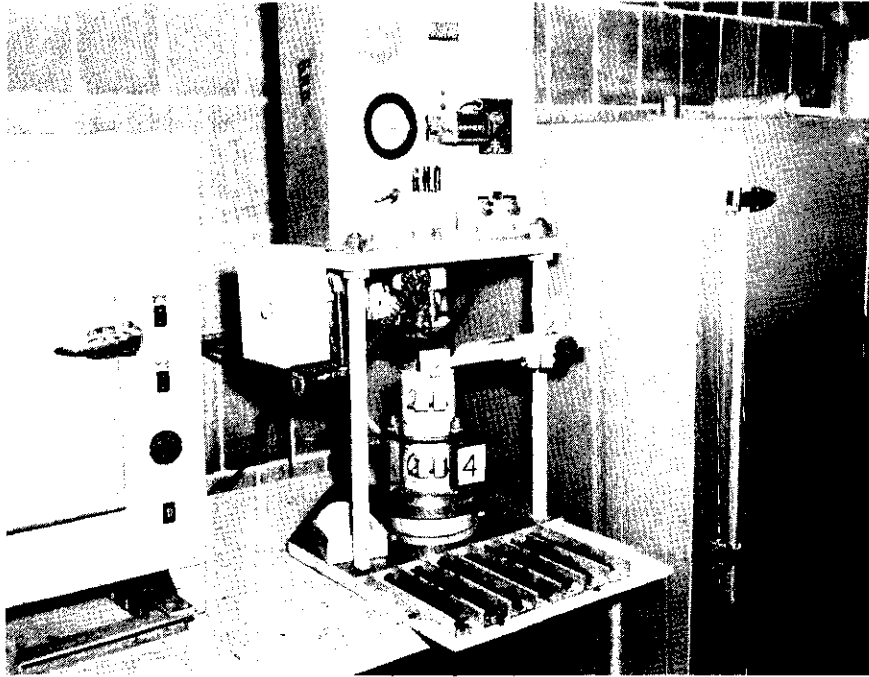


Figure 5. Specimen Compaction Apparatus.

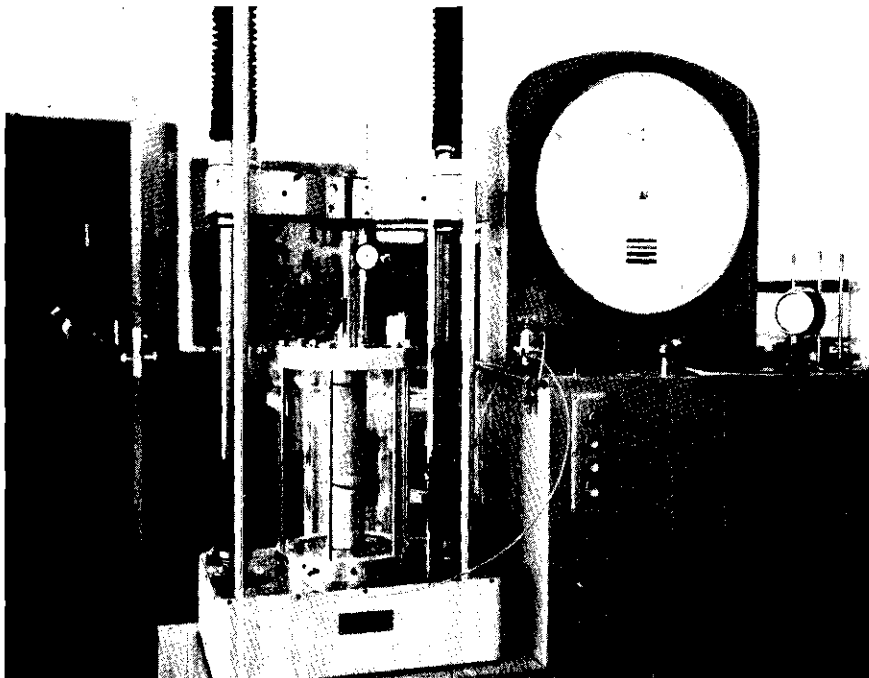


Figure 6. Triaxial Test Apparatus.

## CHAPTER III

## PROCEDURE

General.--Triaxial specimens were batched, mixed, and compacted with asphalt contents of 4, 5, 6, 7, and 8 per cent by weight of dry aggregate. For each asphalt content, duplicate specimens were loaded triaxially at each of three different lateral pressures (10, 20, and 40 psi). Sufficient data was obtained for calculation of density, stress vs. strain curves, the Mohr Diagram components ( $\phi$ ,  $C$ , and  $S_c$ ), per cent void in the total mix, and per cent voids in the mineral aggregate. Test temperature and loading rate employed on these specimens were respectively,  $140^\circ$  F and 0.05 inches per minute. Specimens containing 6 per cent asphalt were triaxially loaded at the same lateral pressures and loading rates, but at temperatures of  $70^\circ$ ,  $35^\circ$ , and  $0^\circ$  F. The effect of temperature and asphalt content on the triaxial properties of angle of internal friction ( $\phi$ ), apparent cohesion ( $C$ ), and unconfined shear strength ( $S_c$ ) were computed and presented in graphical form. (See Appendix III for definitions of  $\phi$ ,  $C$ , and  $S_c$ .)

Aggregate Preparation.--Crushed granite was oven dried and divided into sizes by material retained on 3/4 inch, 3/8 inch, Nos. 4, 8, 16, 30, 50, 100, and 200 sieves and marble aggregate was used for sizes finer than the No. 200 sieve.

Cumulative batch weights for 3800 gram specimens were computed from gradation curves on Figure 5, and each specimen was batched and sealed in a tin container. Although an exact reproduction of this gradation curve could be ascertained only by washing the aggregate through the sieves, the samples batched are at least uniform in gradation. This method presented some control over the amount of fine material in the mix.

Mixing and Curing.--Following overnight storage in a 300° F oven, the aggregate specimen was placed in a mixing bowl, weighed, and a predetermined amount of asphalt was added by weight. The sample was mixed to a uniform consistency with a mixing spoon. Asphalt was only heated enough to attain the mixing temperature (300° F) as a precaution against oxidation. Storage for approximately fifteen hours in open 12 x 18 inch pans in a 140° F forced draft oven preceded compaction.

Compaction.--Compaction was achieved by 250 blows of a kneading compactor at 335 psi foot pressure with a dwell time of 0.36 seconds. The mixture was fed into the 4-inch diameter mold in a uniform manner as the machine operated by schedule shown in Table 1. Prior to compaction, each specimen was heated to 230° F and divided equally into eight aluminum sleeves. Each sleeve was removed from the oven separately and its contents fed into the mold by small increments as the machine operated. Upon completion of one specimen, the

Table 1. Schedule of Compaction Blows for  
4-Inch Diameter Specimen

Part	Blows
0	0
1/8	20
1/4	51
3/8	82
1/2	113
5/8	144
3/4	176
7/8	208
1	240
Leveling	250

next was placed in the eight sleeves and returned to the oven. Next the mold and holder were removed from the compaction machine turntable and the specimen extracted by releasing the split mold's restraining bolts. The mold, holder, and turntable was reassembled and the compaction procedure repeated.

This compaction procedure is based on 250 total blows and the use of a maximum number of blows that could be applied at the top and bottom of the specimen without excessive aggregate crushing. Preliminary tests indicated that no more than 20 blows could be applied to the first 1/8 of the specimen without excessive crushing and no more than 10 leveling blows could be used for the same reason. The remainder of the 250 blows was divided equally to the other seven parts of the specimen.

Bulk Specific Gravity.--Preliminary triaxial tests indicated that paraffin coated samples yield different strength results,

at some temperatures, than uncoated samples. Therefore, it was necessary to establish a correlation between bulk specific gravities obtained from specimens with and without the paraffin coating. This was accomplished by compacting four samples at each asphalt content and determining the bulk specific gravity of each before and after paraffin coating. Prior to paraffin coating, each sample was air dried to a constant weight.

Bulk specific gravities of test specimens were determined by procedures set forth in AASHTO Standard M-132. Formula used for paraffin coated specimen calculation was:

$$\text{Bulk Specific Gravity} = \frac{A}{D - E - \left( \frac{D - A}{F} \right)} \quad (1)$$

where:

- A = weight in grams of the dry specimen in air,
- D = weight in grams of the dry specimen plus paraffin coating in air,
- E = weight in grams of the dry specimen plus paraffin coating in water, and
- F = bulk specific gravity of the paraffin .

The formula used for uncoated specimen calculation was:

$$\text{Bulk Specific Gravity} = \frac{A}{A - C} \quad (2)$$

where:

- A = weight in grams of dry specimen in air, and
- C = weight in grams of dry specimen in water .

Subsequent specimens were not coated with wax for bulk specific gravity determinations, but the corrections in

Table 2 were applied to correct for the water that penetrated the sample when submerged weight was measured.

Table 2. Bulk Specific Gravity Correction  
for Various Asphalt Contents

Asphalt Content	Bulk Specific Gravity Correction
4	- 0.10
5	- .07
6	- .03
7	- .02
8	- .02

Preparation for Triaxial Testing.--Prior to testing, the average height and diameter of each specimen was recorded and a brimsto cap, similar to that used on concrete cylinders, was applied to the top and bottom of the test specimens. The hot fluid was poured into the capping mold, the sample was set into place parallel to the capping mold's vertical guide, and after the cap became solid, the sample was removed. This capping procedure insured that the loading ends would lie in parallel planes and be perpendicular to the specimen's vertical axis. Drainage through the lower cap was facilitated by drilling approximately 25 holes through the cap. The specimens were then wrapped in a paper towel to reduce triaxial membrane breakage due to the sharp aggregate.

Triaxial Testing.--Specimens to be tested at 140° F were placed in a 140 ± 5° F oven for three to four hours prior to testing. Cell fluid used in triaxial chamber was tap

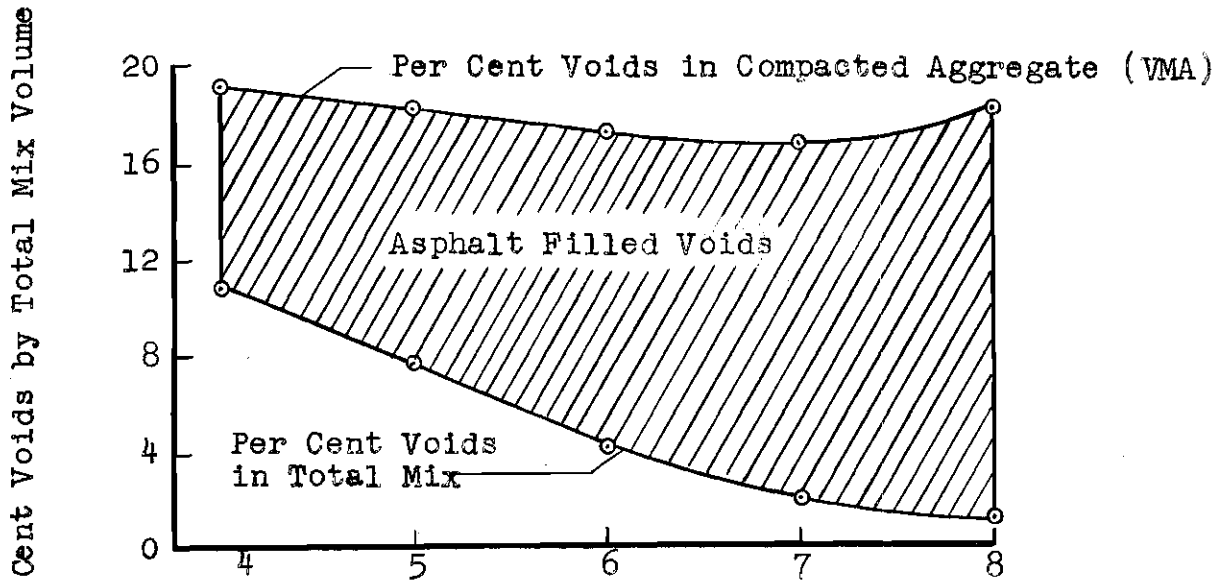
water at 140° F. While the 70, 35, and 0° F test specimens and the cell fluid were stored over night in a freezer, designed to maintain these temperatures within  $\pm 2^\circ$  F. The specimens were removed from their constant temperature air baths separately and placed in the triaxial cell. The sample temperature was controlled by filling the triaxial chamber with fluid. Air pressure was applied in the triaxial chamber and regulated such that the pressure gage on the triaxial cell indicated the desired lateral pressure (10, 20, or 40 psi). After the deflection and load dial gages were zeroed, the sample was deformed at the rate of 0.05 inches per minute. Simultaneous readings of the load dial in pounds and the deflection dial in 0.001 inches were recorded at sufficient increments to plot a well-defined stress vs. strain curve.

Computation of Triaxial Strength Properties.--Values for angle of internal friction ( $\phi$ ), apparent cohesion (C), and unconfined shear strength ( $S_c$ ) were computed for each series of tests. For a more detailed account of these calculation procedures, see Appendix III. A comparison of the values of these terms under conditions of changing asphalt contents and temperatures are shown in Chapter IV.

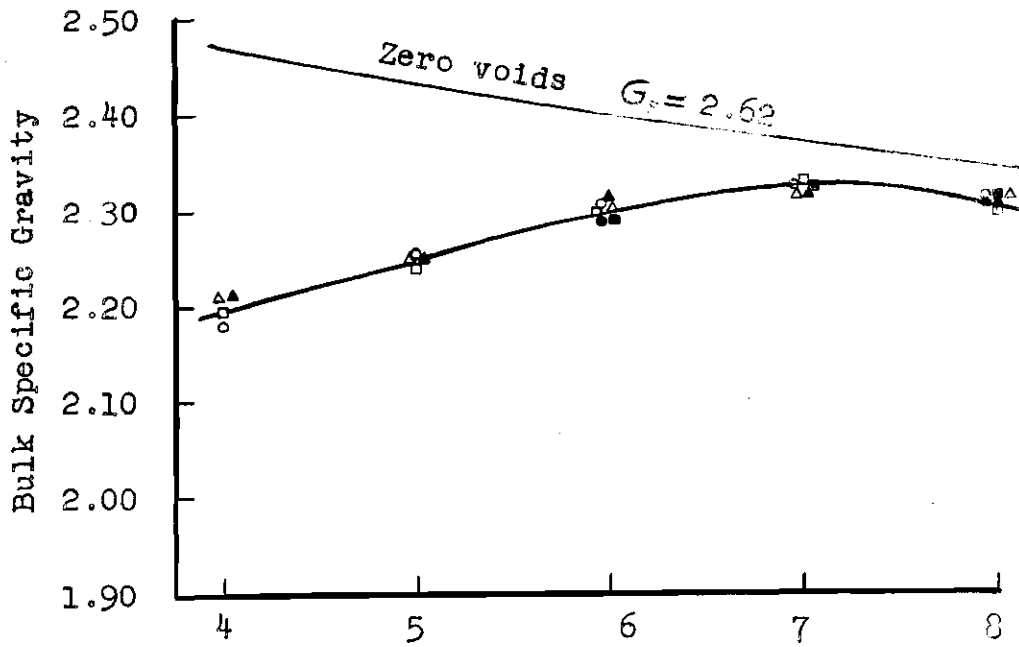
## CHAPTER IV

## RESULTS

Compaction and Asphalt Content.--The effect of asphalt content variation on compaction is illustrated in Figures 7 and 8. The addition of each increment of asphalt from 4.0 to 6.0 per cent resulted in a uniform increase in the bulk specific gravity of the mix and uniform decreases in the per cent voids in the total mix and per cent voids in the compacted aggregates. The reduction of voids in the total mix was 6.6 per cent while the reduction in voids in the compacted mineral aggregate was only 2.0 per cent. This indicates that only about one third of this increase in bulk specific gravity resulted from aggregate voids with asphalt. At 7.0 per cent asphalt the bulk specific gravity of the compacted sample reached a maximum of 2.33 and dropped back to 2.32 at 8.0 per cent asphalt. Over the same increment, the voids in the total mix continued to reduce, but at a decreasing rate and appear to approach a limit of about one per cent. Now the per cent voids in the compacted aggregate drops slightly to a minimum of 16.8 per cent and swings sharply back up to 18.2 per cent. Apparently the sample becomes flooded with binder between the asphalt contents of 7.0 and 8.0 per cents and the lubrication afforded by the asphalt allows the aggregate to attain the most desirable orientation



Per Cent Asphalt by Dry Aggregate Weight  
 Figure 7. Per Cent Voids vs. Asphalt Content Curves.



Per Cent Asphalt by Dry Aggregate Weight  
 Figure 8. Bulk Specific Gravity vs. Asphalt Content

at an asphalt content of about 7.0 per cent. Monismith and Vallerga (9) conducted compaction tests on an aggregate of this gradation at identical asphalt contents. Their results indicate that increasing compactive effort lowers the amount of asphalt necessary to attain maximum density. This asphalt content at maximum density must be considered then in terms of the compaction effort used. A greater compaction effort will yield maximum density at a lower asphalt content.

Angle of Internal Friction and Asphalt Content.--Figure 9 illustrates the effect of asphalt content on the angle of internal friction of this mix at 140° F. This angle increases almost linearly to a peak at 7.0 per cent asphalt and drops back to 45 degrees at 8.0 per cent asphalt. The shape of this curve compares almost identically with the VMA vs. asphalt content curve if one of the curves are inverted. This relationship is further exhibited in Figure 11 where per cent voids in the compacted mineral aggregate plotted as a linear function of the angle of internal friction. Since the voids between the compacted aggregate particles is a measure of the amount of compaction experienced by the aggregate, regardless of asphalt content; it is reasonable to conclude that the friction angle for this mix is a function of the degree of compaction experienced by the aggregate.

Shear Strength and Asphalt Content.--The shear stress along the plane of rupture, just prior to failure of the specimen, when no external lateral pressure is termed unconfined shear strength decreases along a convex curve of uniform curvature

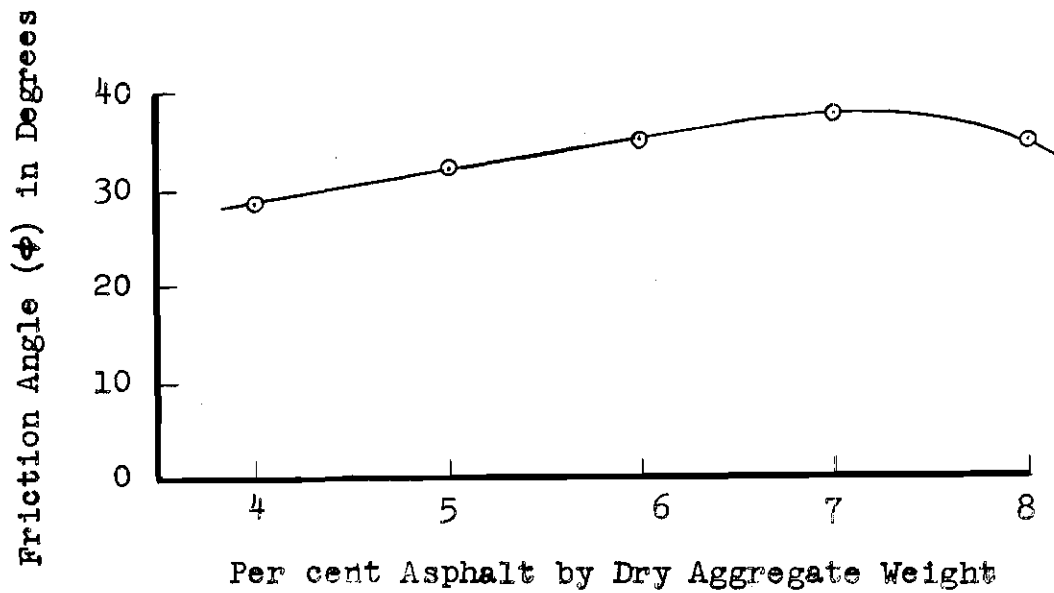


Figure 9. Angle of Internal Friction vs. Asphalt Content from Tests at 140° F.

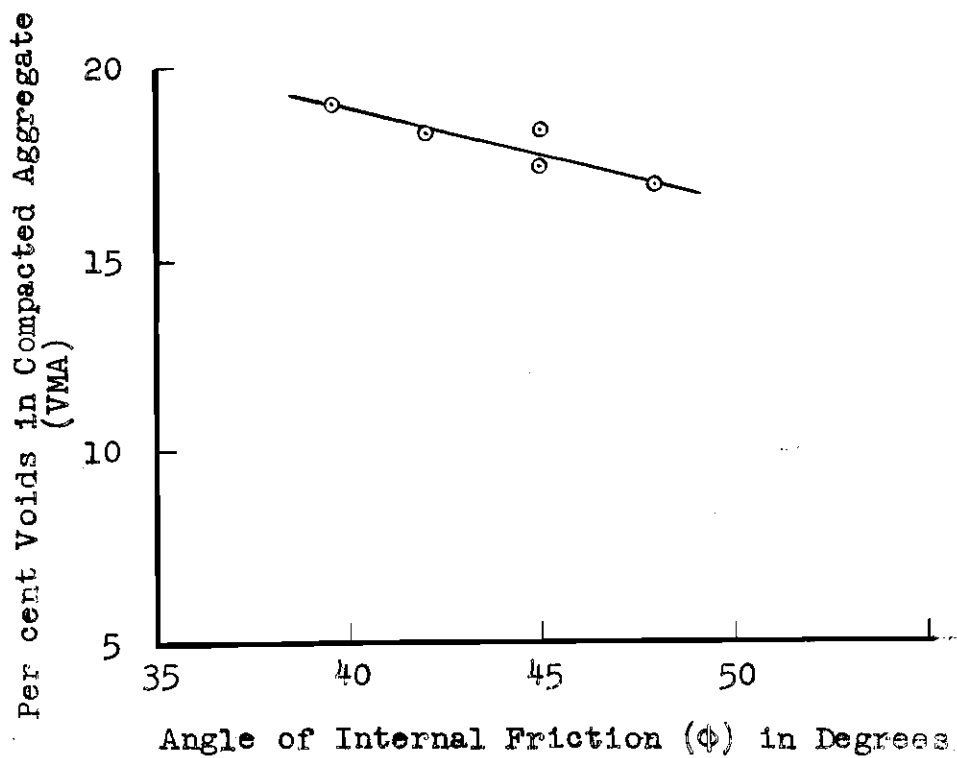


Figure 10. The Effect of Compaction on the Angle of Internal Friction of Specimens Tested at 140° F.

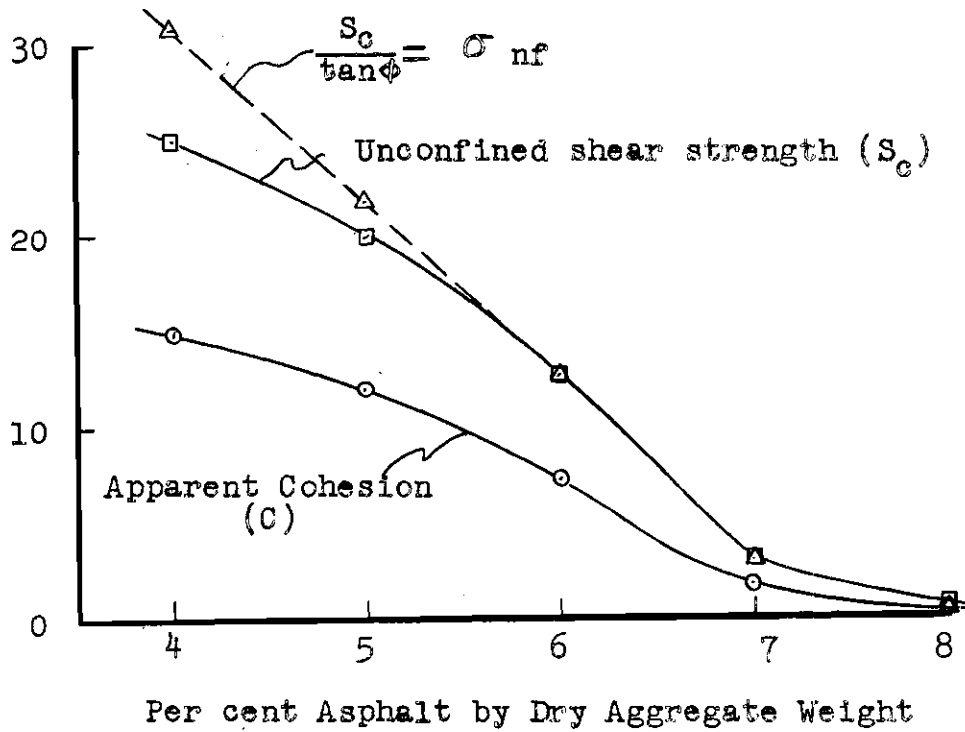


Figure 11. Unconfined Shear Strength ( $S_c$ ) and Apparent Cohesion ( $C$ ) vs. Asphalt Content Curves at 140° F.

as the asphalt content increases from 4.0 per cent to approximately 7.0 per cent. Here the trend seems to reverse to a flatter slope and descends to a shear stress of 0.7 psi at 8.0 per cent asphalt. The bulk specific gravity curve (Figure 8) and VMA curve (Figure 7) indicate a condition of maximum compaction at about 7.0 per cent asphalt and experience indicates that this is caused by the asphalt reaching a practical limit for this aggregate or near flooded conditions. Here fluid pressures prevent further compaction and increasing asphalt contents beyond 8.0 per cent were impossible since the fluids prevented sufficient particle contact to form a cohesive sample. The abrupt change in the curve could have indicated a near saturated condition.

The segment of the unconfined shear strength vs. asphalt content relation between 4 per cent and 7 per cent has a convex shape which may be eliminated by removing the effect of a changing friction angle. Since shear stress on a plane is a function of the friction angle and the normal stress, then the normal stress on this plane will be an equivalent index. This unconfined normal stress, computed from equation (3) is shown (Figure 11) to vary linearly with asphalt contents between 4.0 per cent and 7.0 per cent.

$$\sigma_{nf} = \frac{S_c}{\tan \phi} \quad (3)$$

where

$\sigma_{nf}$  = the normal stress on the rupture plane of a triaxial specimen with no lateral support ( $\sigma_3 = 0$ ), at the maximum load attained by the specimen,

$S_c$  = the shear stress on the plane of rupture at the maximum load attained by the specimen, and

$\tan\phi$  = the slope of the Mohr rupture line .

One explanation for this linear relationship between unconfined normal stress and asphalt content is related to the surface tension properties of the asphalt at relatively high temperatures, 140° F in this case. At say 4.0 per cent asphalt a specimen is molded with a certain volume of voids within the mineral aggregate. Then the asphalt must have a certain amount of "fluid to air" surface area. If surface tension forces tend to pull the aggregate particles together, then a normal stress must be induced at aggregate contact points that is governed by the shape, size, and number of the void spaces around the points. This is true since surface tension force on a solid is a function of the fluid surface's curvature. Now if an equivalent specimen contains sufficient asphalt to fill some of these voids and thereby destroy the surfaces, the normal stress at contact points must decrease. In Figure 11, the asphalt is added by weight of dry aggregate, then constant volume increments are added to the mix in this illustration. Because filling the voids is also a volumetric function, then it stands to reason that the unconfined normal stress will decrease.

linearly as voids in the compacted aggregate are progressively inundated. An important point to keep in mind when determining unconfined normal stress is the viscosity of the asphalt. For the above analysis to be valid, the sample must be deformed at a rate slow enough to eliminate viscous shear of the asphalt film. There are two properties of fluids to be considered, viscosity and surface tension. Both variables are believed to take place but at high temperatures and slow loading rates, viscosity shear forces are quite small for most paving grades of asphalt.

Angle of Internal Friction and Temperature.--Figure 13 illustrates the effect of temperature on the angle of internal friction or the angle subtended by the horizontal axis and rupture line of the Mohr diagram. This data was computed from trend curves (Figure 26) of failure stress at various lateral pressures with variation of temperature.

As test temperature was increased from  $10^{\circ}$  F the angle values decreased from 54 degrees to a minimum of 25 degrees at  $60^{\circ}$  F. The curve then ascended at about the same value of slope to about  $100^{\circ}$  F where the trend tends to flatten and approach a horizontal asymptote of angle of internal friction equal to 45 degrees.

Since asphaltic concrete pavement is composed of a viscous liquid and a cohesionless solid, the properties of both ingredients must determine the characteristics of the mixture. Shear strength for cohesionless material is chiefly attributed

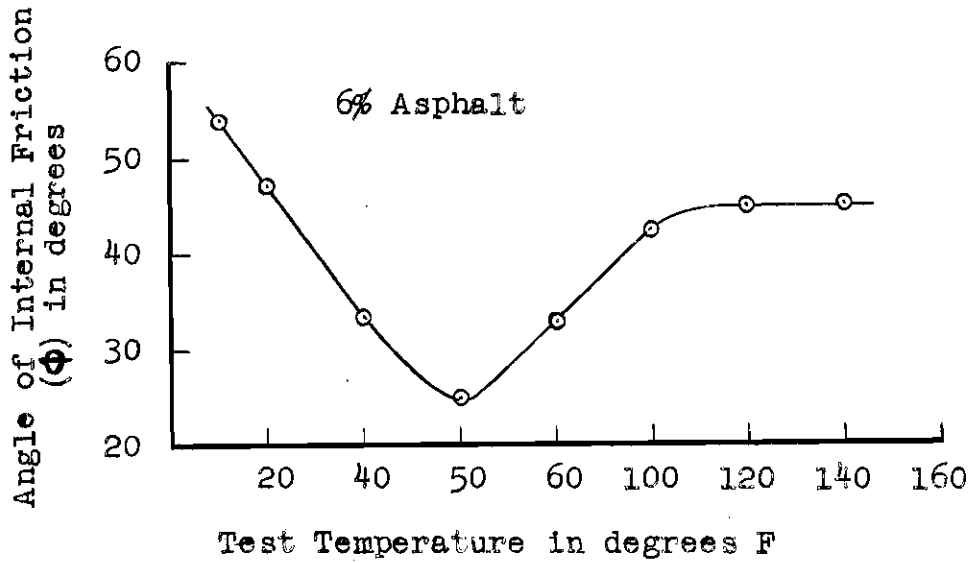


Figure 12. The Effect of Temperature on the Angle of Internal Friction of Specimens Containing 6 Per Cent Asphalt.

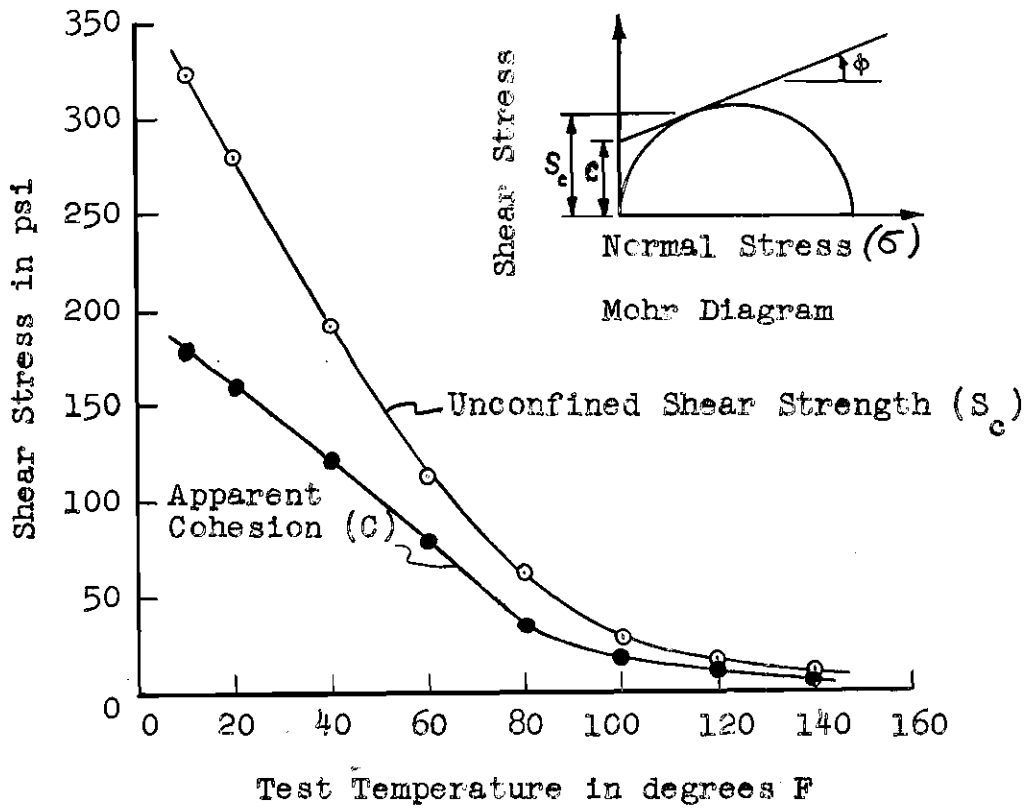


Figure 13. The Effect Test Temperature on Unconfined Shear Strength and Apparent Cohesion of Speciment Containing 6 Per Cent Asphalt.

to aggregate contact points and the shear generated at a particular contact point is proportional to the pressure forcing the points together. The performance of liquids having high internal friction or viscosity is usually described by referring to the movement of two plates separated by the liquid in question. Under these conditions, the resistance of the liquid is virtually independent of pressure, but varies directly with the area and directly with the speed of movement. Then any characteristic of a pavement of this type must be a combination of these two different materials unless special test conditions reduce the influence of some of these component characteristics.

The variation of the angle of internal friction shown in Figure 14 may be explained as the resultant of two opposite effects caused by decreasing viscosity of the binder as the temperature rises. Decreasing viscosity with increasing temperature results in a gradual transformation of the binder from a solid to a semi-solid and finally to a fluid. When the binder is a solid, the amount of shear force transferred from one aggregate point to another is a function of the normal pressure between the points but when the binder is a fluid, the amount of shear transmitted is a function of the binders viscosity, not the normal pressure. Now decreasing viscosity also allows more aggregate points to penetrate the separating binder films and strength derived from aggregate point contact is a function of the normal pressure; thus,

one effect seems to cancel the other at about 60° F. Viscosity decreases, resulting from increases in temperatures, continue to allow more and more aggregate contact points until the shear due to viscous forces is small compared to friction forces of the aggregate. Further reduction in viscosity at temperatures above about 100° F effect little change in the angle of internal friction; hence, this value is considered a measure of this mix's aggregate's frictional property alone. Note that a combination of high test temperature and slow deformation rate is necessary to eliminate viscosity effects of the binder.

Shear Strength and Temperature.--Shear stress at rupture for unconfined compression of a 6.0 per cent asphaltic concrete pavement is illustrated in Figure 13, like Figure 12, this is an illustration of a trend which was derived from the family of curves on Figure 28. Values for unconfined shear strength decrease as a linear function of temperature increase from 324 psi at 10° F to 150 psi at 50° F. This shear stress then continues to reduce as temperature increases, but at a progressively slower rate between the temperatures of 50 and 100° F until the curve seems to approach a constant slope between 100 and 140° F.

The unconfined shear strength is a measure of the specimens viscous shear resistance and frictional resistance due to internal normal pressure (surface tension) on the plane of rupture. Viscous shear is considered the predominant

factor in the unconfined shear strength (Figure 13) up to temperatures of about 80° F. Between 80 and 140° F the shear vs. temperature gradually approaches a constant slope. This slope is considered a function of surface tension variation with temperature. The constant angle of internal friction between 110 and 140° F substantiates an absence of viscous effects.

Stress and Deformation.--An important consideration for a good asphalt pavement is the amount of deformation the material must sustain to support a given applied load. Figure 14 illustrates the effect of asphalt content on the ability of this asphalt concrete to support load at strains of 0.5, 1.0, and 1.5 per cent. The values of stress indicated for 1.5 per cent strain are very close to the ultimate stress values for 8.0 per cent asphalt is only about one-half that ultimate stress. This is an important consideration in pavement design since impractical amounts of deformation is required for a rich mix to accommodate ultimate load.

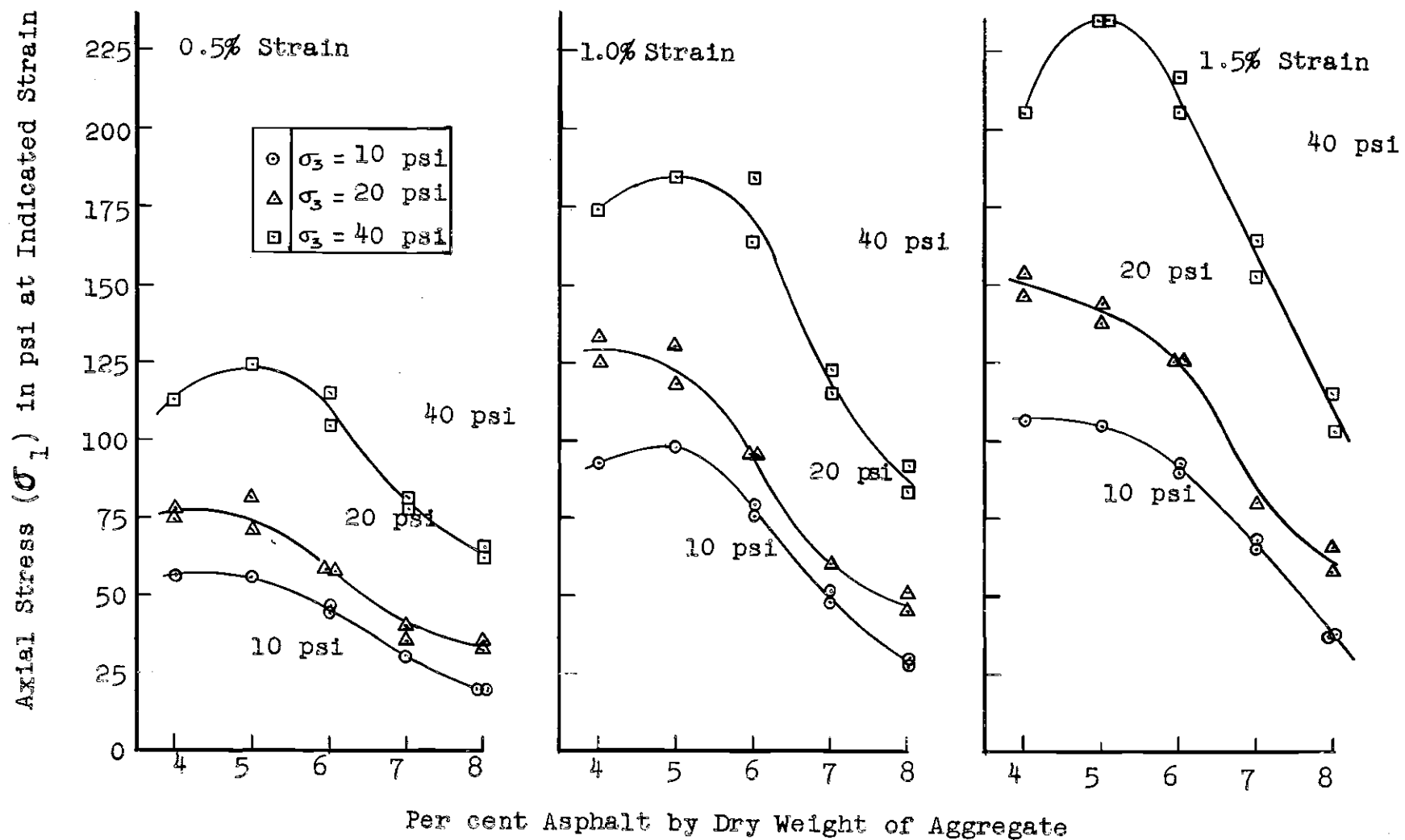


Figure 14. Axial Stress ( $\sigma_1$ ) vs. Asphalt Content for Lateral Pressure ( $\sigma_3$ ) of 10, 20 and 40 psi at 0.5, 1.0, and 1.5% Strain. Test Temperature is 140° F.

## CHAPTER V

## CONCLUSIONS AND RECOMMENDATIONS

- Conclusions.--(1) The point of maximum compaction was defined at about 7.0 per cent asphalt by weight of aggregate.
- (2) This particular paving mixture seems to exhibit an angle of internal friction that is directly dependent on the percentage of voids existing in the mix, including that volume occupied by the asphalt.
- (3) The shear strength at zero lateral pressure decreases as asphalt content is increased from the leanest mixtures to the point of maximum compaction.
- (4) After cancelling the effect of changing friction angle, the above property reduces in direct proportion to the volume of asphalt added to the mix between the lowest asphalt contents and the point of maximum compaction.
- (5) The rate of strain used in this research is sufficiently slow to remove the effect of viscous shear on this pavement's angle of internal friction if tests are conducted at temperatures above 120° F.
- (6) Reduction in test temperature between 100 and 60° F effected decreasing angle of internal friction values while further reduction to 10° F resulted in increasing values.

(7) Specimens containing 4.0, 5.0, and 6.0 per cent asphalt generally reaches ultimate stress around 1.5 per cent strain.

(8) Increased lateral support and asphalt content increased the amount of strain required for rupture.

Recommendations.--(1) An extension of this research into many different types of pavements is necessary to determine if the relationships derived from this research apply to several types of asphalt concrete pavements.

(2) Improvement and standardization of compaction methods, using a kneading compactor, would greatly aid the field of asphalt pavement research.

(3) A study of the shape of Mohr envelopes for various paving mixtures would greatly aid the pavement designer.

A P P E N D I C E S

## APPENDIX I

## VOIDS ANALYSIS PROCEDURE (10)

The maximum theoretical bulk specific gravity,  $D$ , was determined for each asphalt content from the batch weights and bulk specific gravities of the mix ingredients.

$$D = \frac{W_1 + W_2 + W_3}{\frac{W_1}{G_1} + \frac{W_2}{G_2} + \frac{W_3}{G_3}} \quad (4)$$

where  $W_1$ ,  $W_2$ , and  $W_3$  are the batch weights of the crushed stone, mineral filler, and asphalt, while  $G_1$ ,  $G_2$  and  $G_3$  represents their respective bulk specific gravities. The per cent voids in the total mix,  $V$ , was then computed from the theoretical maximum bulk specific gravity and the average bulk specific gravity of the test specimens for each asphalt content.

$$V = \frac{100 (D - G)}{D} , \quad (5)$$

where:

$D$  = the theoretical maximum bulk specific gravity, and  
 $G$  = the average bulk specific gravity for each asphalt content .

The per cent voids in the compacted aggregate, (VMA), was computed from the theoretical bulk specific gravity of the compacted aggregate, ( $d$ ), and the bulk specific gravity

of the compacted aggregate, (g), in the test specimens. The theoretical gravity was computed by using formula - but excluding asphalt weights and gravities from the calculation. The bulk specific gravity of the compacted aggregate in the test specimen must be proportional to the per cent aggregate contained therein. Then the following relation must exist:

$$g = \frac{W_1 + W_2 + W_3}{W_1 + W_2} G, \quad (6)$$

where:

- G = the bulk specific gravity of the compacted specimen,
- g = the bulk specific gravity of the compacted aggregate,
- W<sub>1</sub> = batch weight in grams of crushed stone in the mix,
- W<sub>2</sub> = batch weight in grams of mineral filler in the mix, and
- W<sub>3</sub> = batch weight in grams of asphalt in the mix .

The per cent voids in the compacted aggregate, (VMA), was then computed from the theoretical maximum specific gravity of the compacted aggregate (d) and the bulk specific gravity of the compacted aggregate (g) by the following relationship:

$$VMA = \frac{100 (d - g)}{d} .$$

Results of these calculations appear in Figure 7.

## APPENDIX II

STRESS AND STRAIN CALCULATION PROCEDURE AND CURVES  
PROCEDURE

The data obtained from each triaxial test was converted into a stress versus strain curve. Simultaneous dial and load readings were plotted and a curve was drawn through the points. The lower section of this curve was extended back to zero load to determine the dial reading at zero deformation. The dial reading at zero deformation was subtracted from each recorded dial reading to obtain the specimen's deformation and this was converted to strain in inches per inch by dividing deformation by the specimen's initial height. The specimen's end area was corrected for bulging during loading by the specimen's initial height. The specimen's end area was corrected for bulging during loading by the following formula:

$$A' = \frac{A}{1 - E} \quad (7)$$

where:

A' = new loaded area in square inches,  
 A = the specimens initial end area in square inches,  
 and E = the computed strain in inches per inch for each load reading.

Then the differential stress for each load reading was computed by dividing the load by the corresponding new area.

The pressure acting on the specimen's top was not added at this time. The axial stress plotted on stress versus strain curves was a differential stress ( $\sigma_1 - \sigma_3$ ).

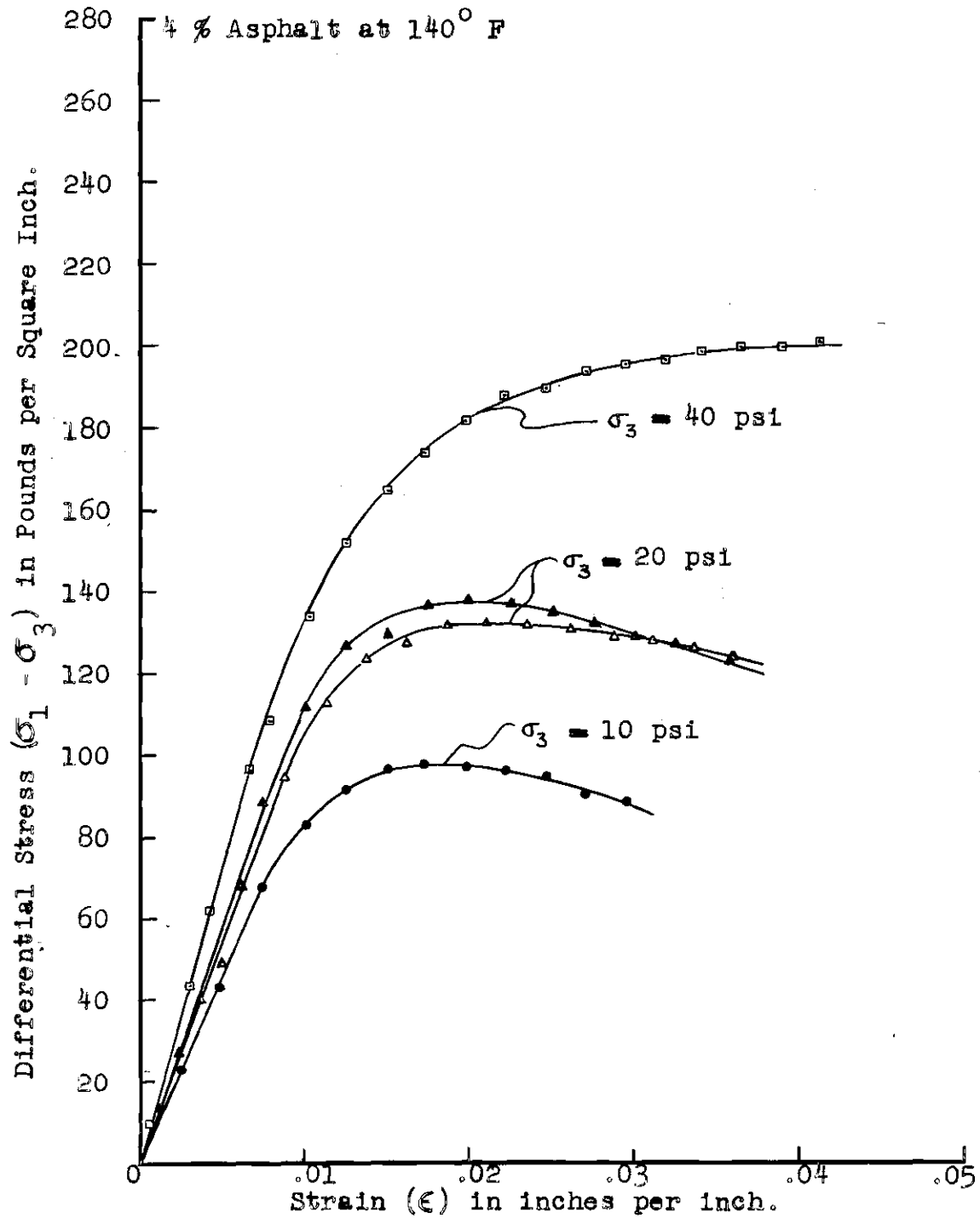


Figure 15. Differential Stress vs. Strain Curves for Specimens Containing 4 per cent Asphalt at 140° F.

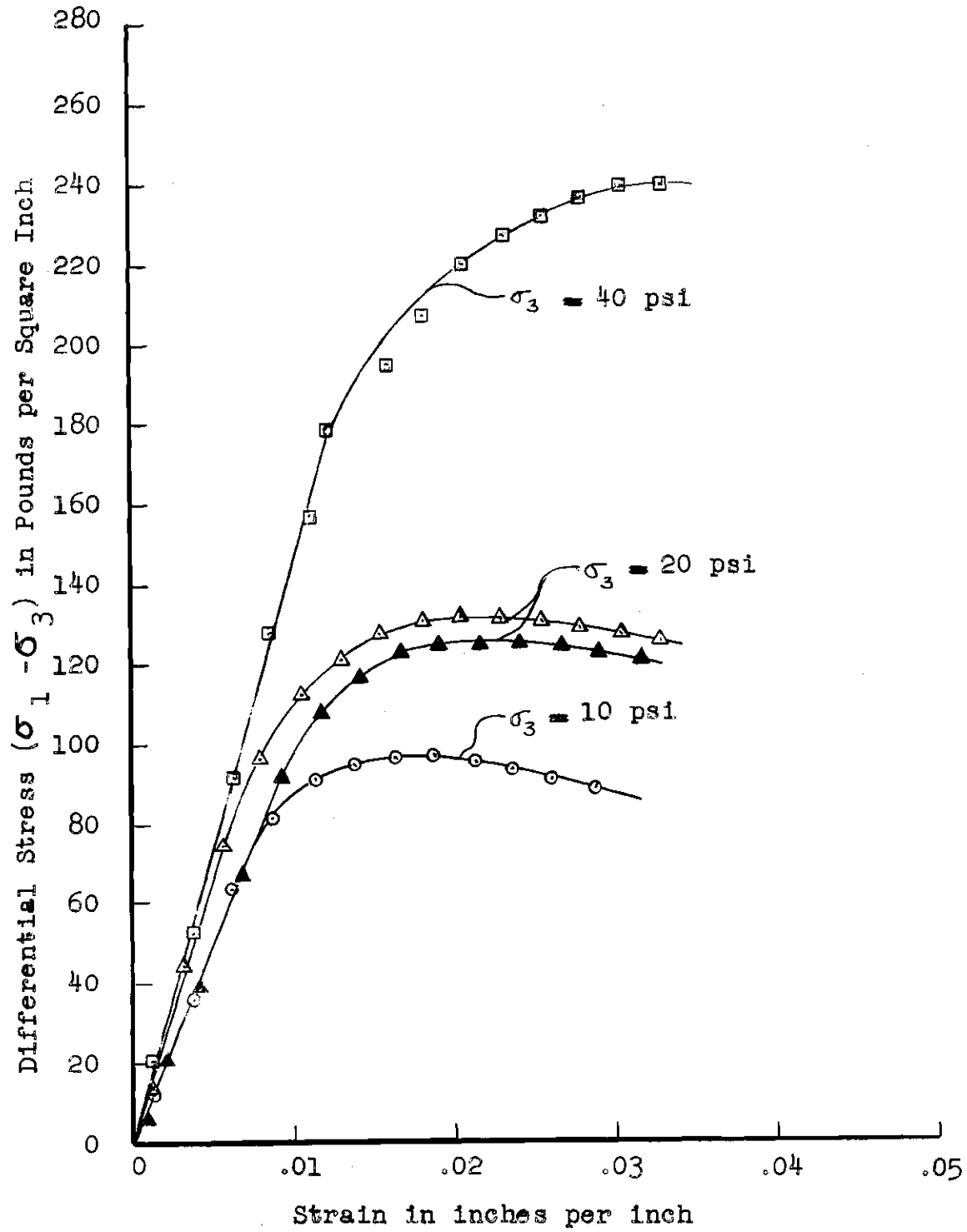


Figure 16. Differential Stress vs. Strain Curves for Specimens Containing 5 per cent Asphalt at 140° F.

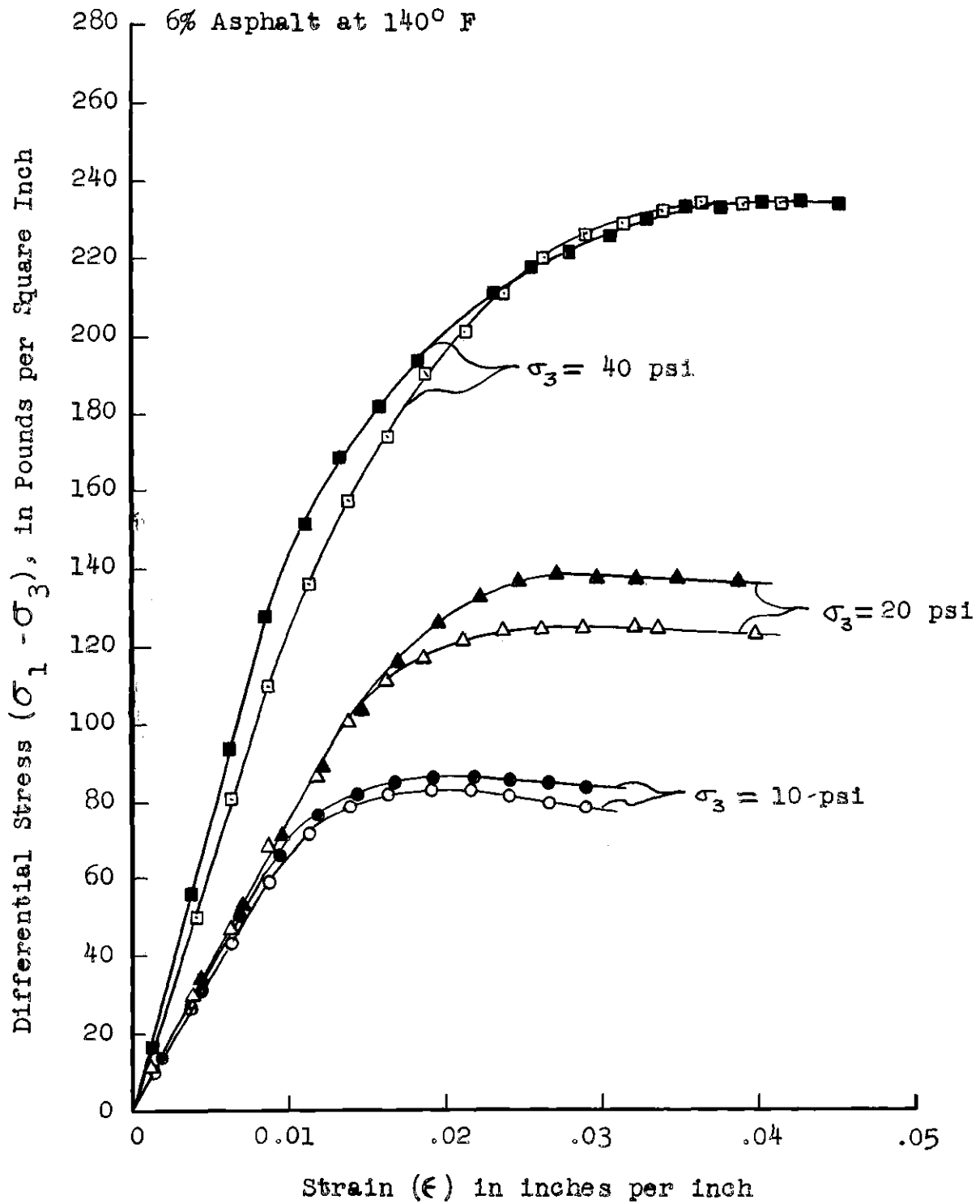


Figure 17. Differential Stress vs. Strain Curves for Specimens Containing 6.0 per cent Asphalt at 140° F.

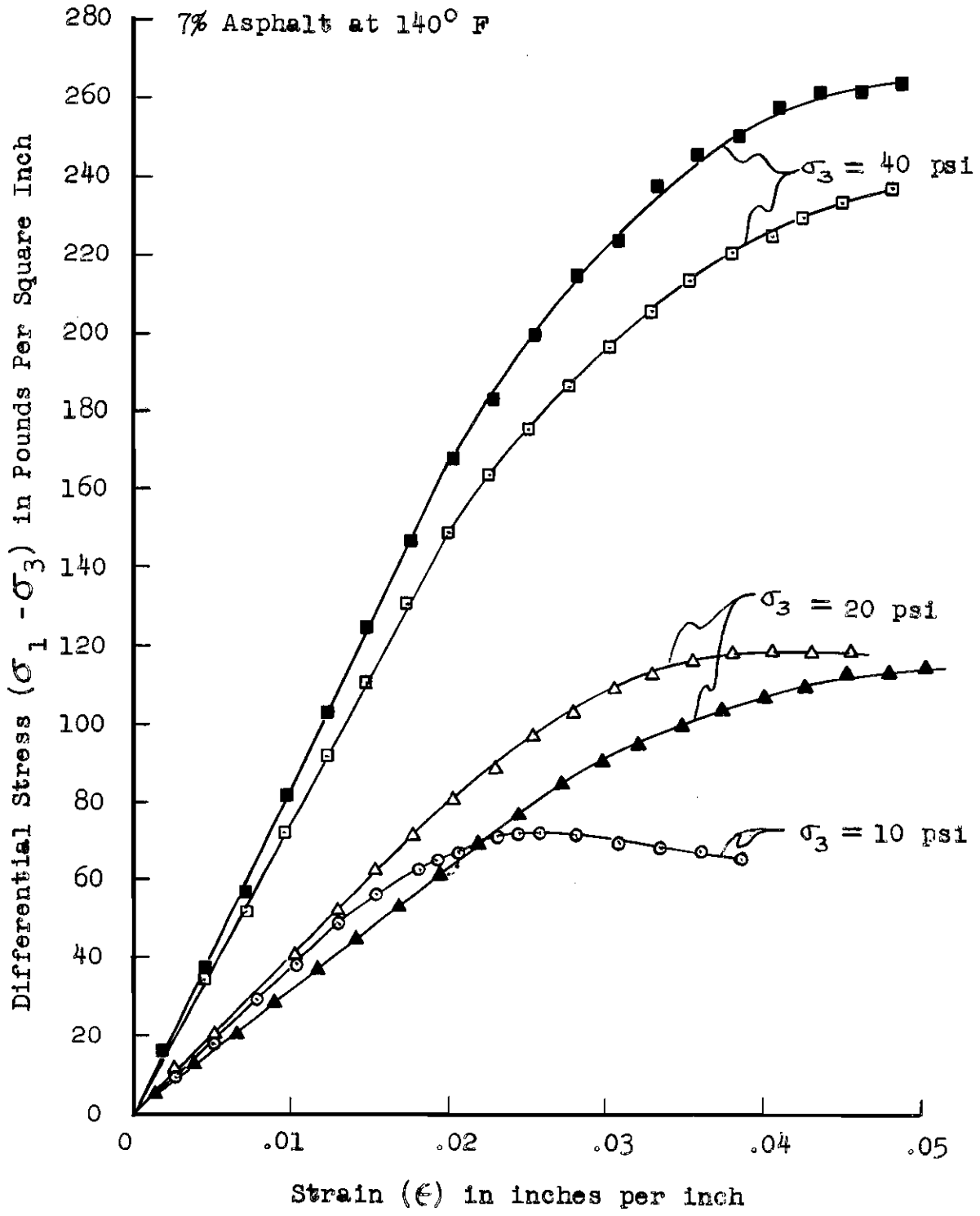


Figure 18. Differential Stress vs. Strain Curves for Specimens Containing 7.0 per cent Asphalt at 140° F.

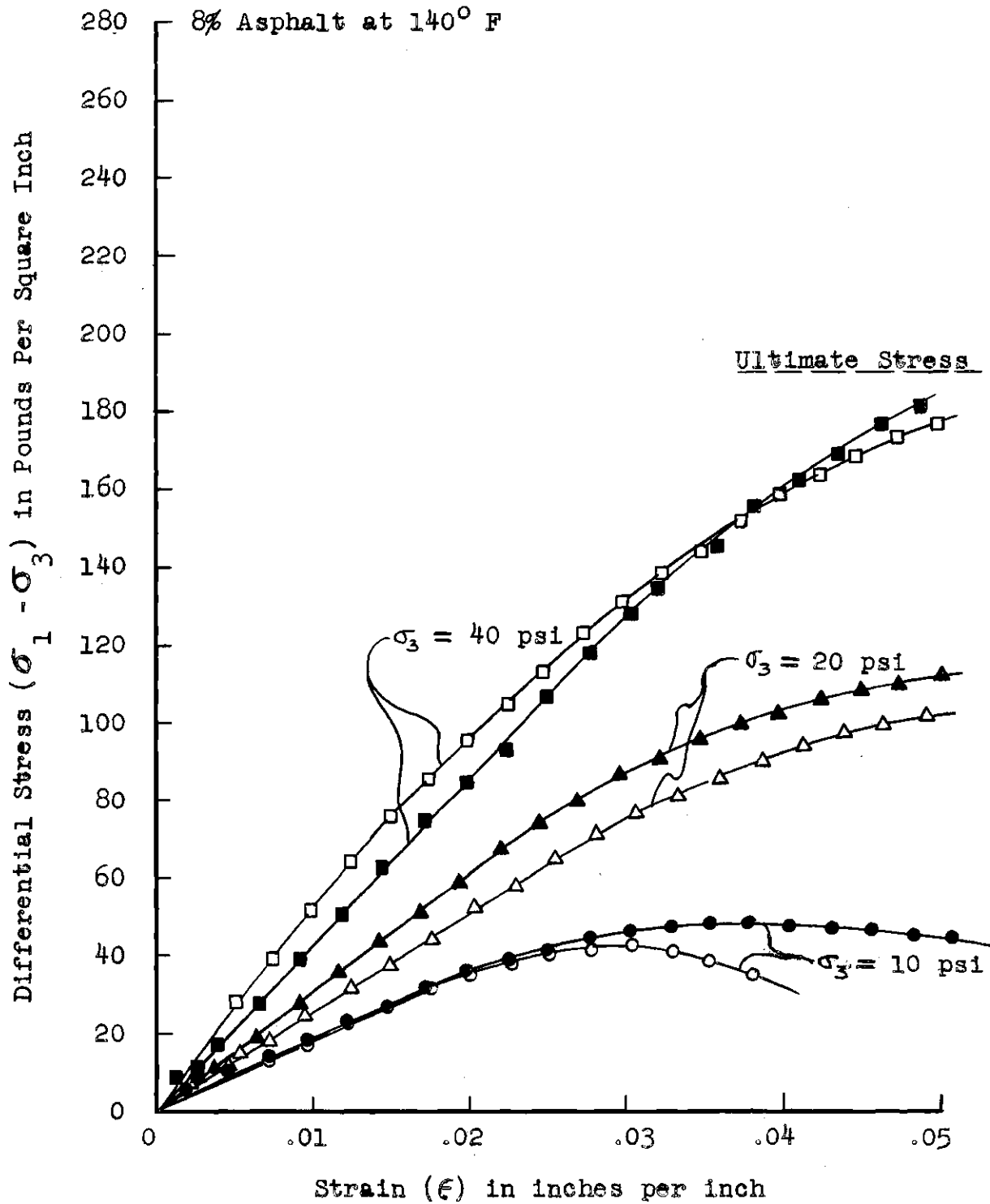


Figure 19. Differential Stress vs. Strain Curves for Specimens Containing 8.0 per cent Asphalt at 140° F.

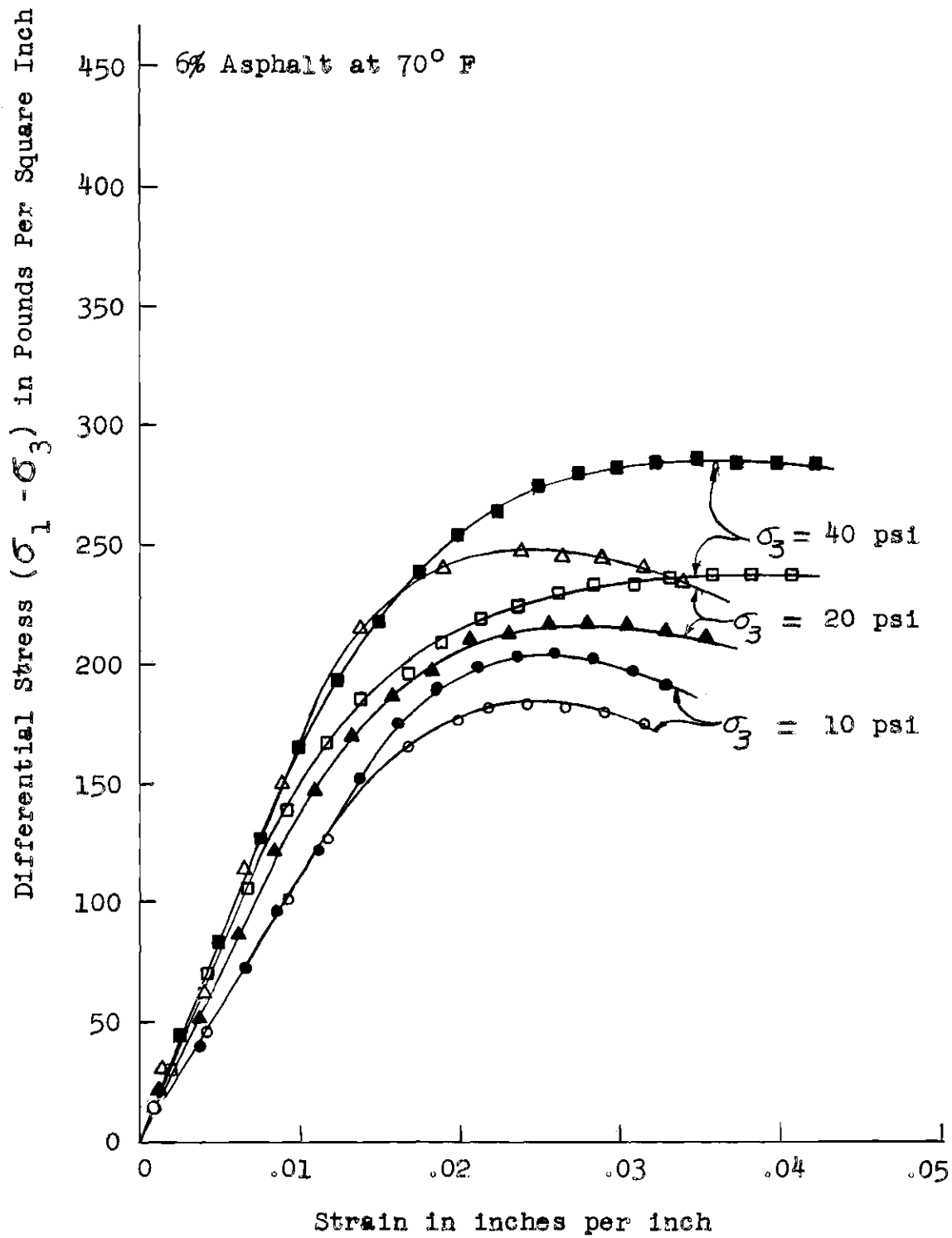


Figure 20. Differential Stress vs. Strain Curves for Specimens Containing 6.0 per cent Asphalt at 70° F.

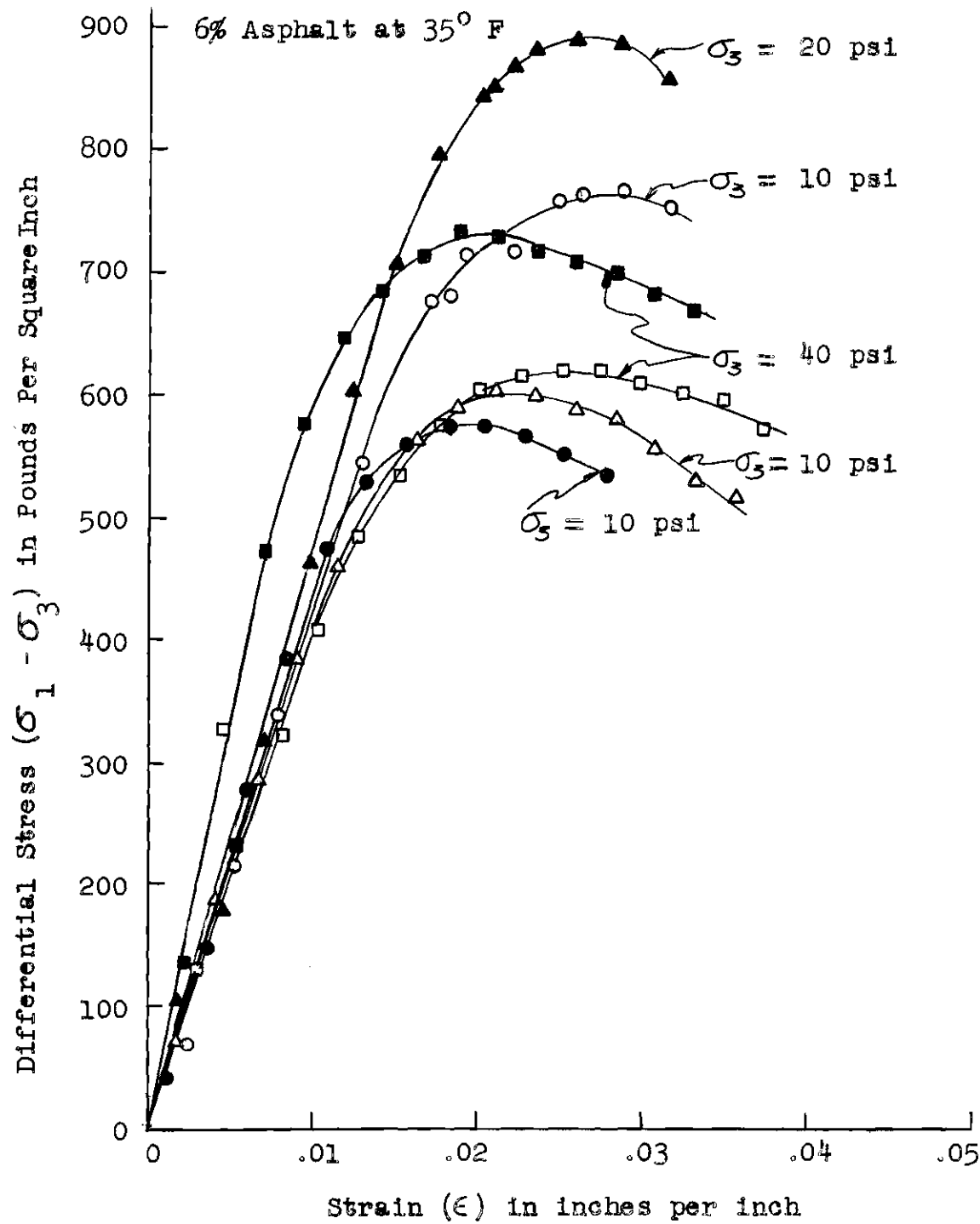


Figure 21. Differential Stress vs. Strain Curves for Specimens Containing 6.0 per cent Asphalt at 35° F.

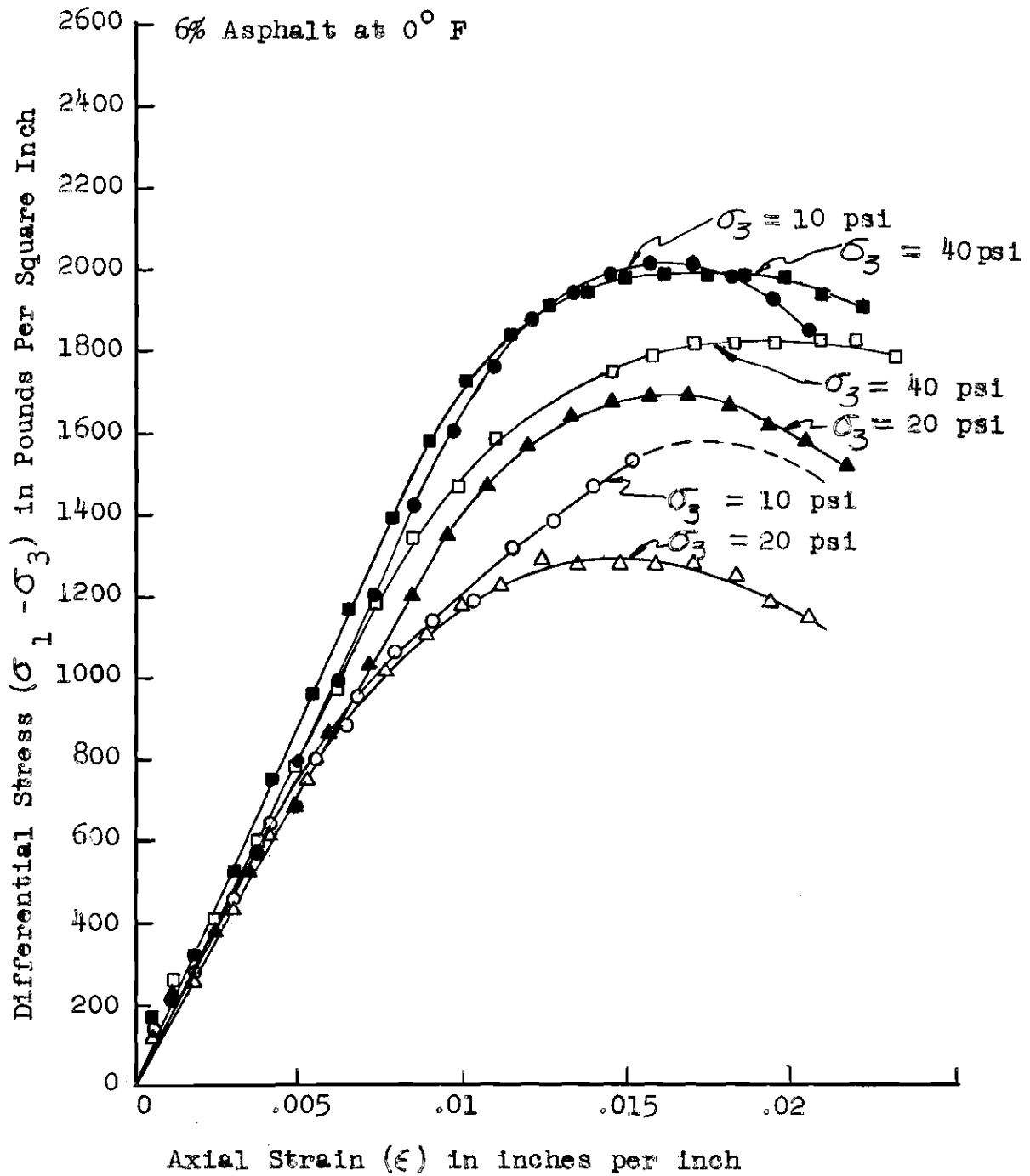


Figure 22. Differential Stress vs. Strain Curves for Specimens Containing 6.0 per cent Asphalt at 0° F.

## APPENDIX III

## CALCULATION OF MOHR DIAGRAM COMPONENTS

The values for apparent cohesion (C) and angle of internal friction are normally determined graphically from the Mohr rupture envelope (Figure 3) by drawing stress circles and constructing a tangent to these circles. However, difficulty sometimes arises when a line must be constructed tangent to several circles that result from experimental differences in Laboratory test data. A more realistic method for determining these index properties has been developed for materials with straight rupture lines.

This method involves plotting results from triaxial tests on an ultimate axial stress ( $\sigma_1$ ) vs. Lateral Pressure ( $\sigma_3$ ) graph (Figure 25). Here a line may be drawn through the data points by the method of least squares and the slope of this line will yield sufficient information for a determination of the angle of internal friction. An expression (9) may be derived from the geometry of a straight rupture envelope that expresses the first principal stress ( $\sigma_1$ ) in terms of lateral pressure ( $\sigma_3$ ), angle of internal friction ( $\phi$ ) and cohesion (C).

$$\sigma_1 = \sigma_3 \tan^2 (45 + \phi/2) + 2C \tan (45 + \phi/2) . \quad (8)$$

Differentiation of this equation yields the following expression for the slope of the  $\sigma_1$  vs.  $\sigma_3$  curve in terms of the angle of internal friction ( $\phi$ ):

$$\frac{d\sigma_1}{d\sigma_3} = \tan^2 (45 + \phi/2) . \quad (9)$$

and solution of equation 8 for zero lateral pressure yields

$$\sigma_1 = 2c \tan (45 + \phi/2) . \quad (10)$$

where  $I$  is the intercept of the  $\sigma_1$  axis and of the  $\sigma_1$  vs.  $\sigma_3$  relation (Figure 25); then,

$$c = \frac{I}{2 \tan (45 + \phi/2)} . \quad (11)$$

Another important index property of an asphaltic concrete mix is the shear stress on the plane of failure when no external support is applied to the specimen. This value is defined as the point of tangency between the rupture line and a stress circle drawn through the origin of a Mohr Diagram. Like apparent cohesion and angle of internal friction, it may be solved graphically or by the geometry of a Mohr rupture envelope. This unconfined shear strength ( $S_c$ ) may be expressed in terms of the angle of internal friction and the ultimate axial stress ( $\sigma_1$ ) where lateral pressure equals zero.

$$S_c = \frac{\sigma_1}{2} \cos \phi \quad \text{if } \sigma_3 = 0 . \quad (12)$$

Then Mohr Diagram components: angle of internal friction ( $\phi$ ), apparent cohesion (C), and unconfined shear strength ( $S_c$ ) were computed from triaxial data with application of equations 5, 7, and 8 respectively. Figures 25, 26, 27, 28 and 29 were used to obtain necessary data to compute these properties by using the indicated formulas.

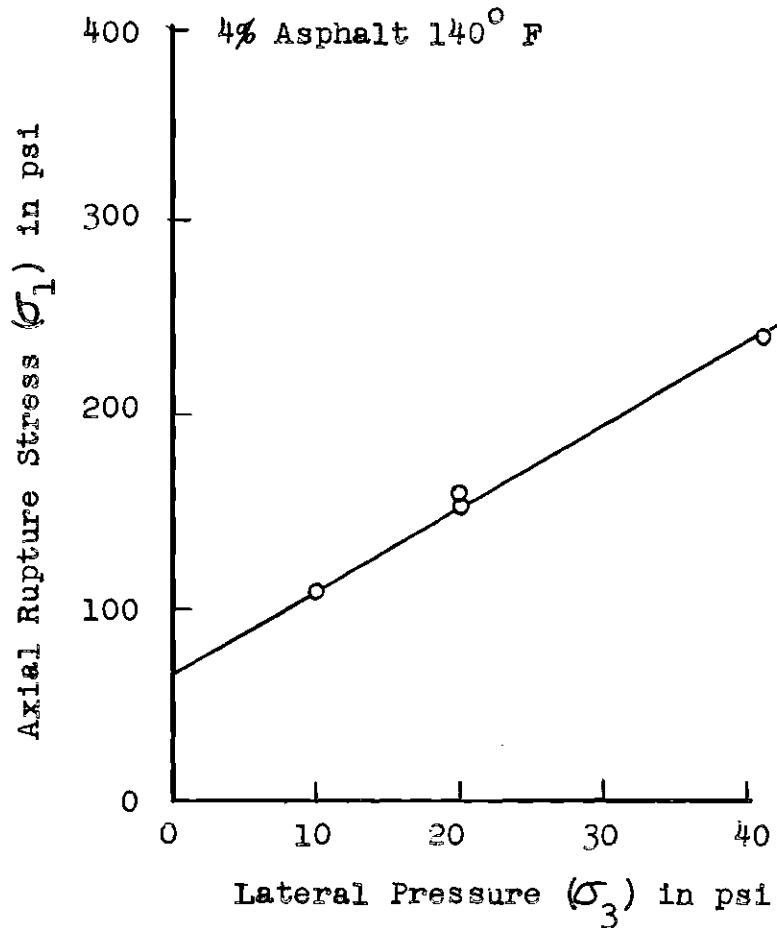


Figure 23. Axial Stress at Rupture vs. Lateral Pressure for Specimens Containing 4.0 per cent Asphalt at 140°F.

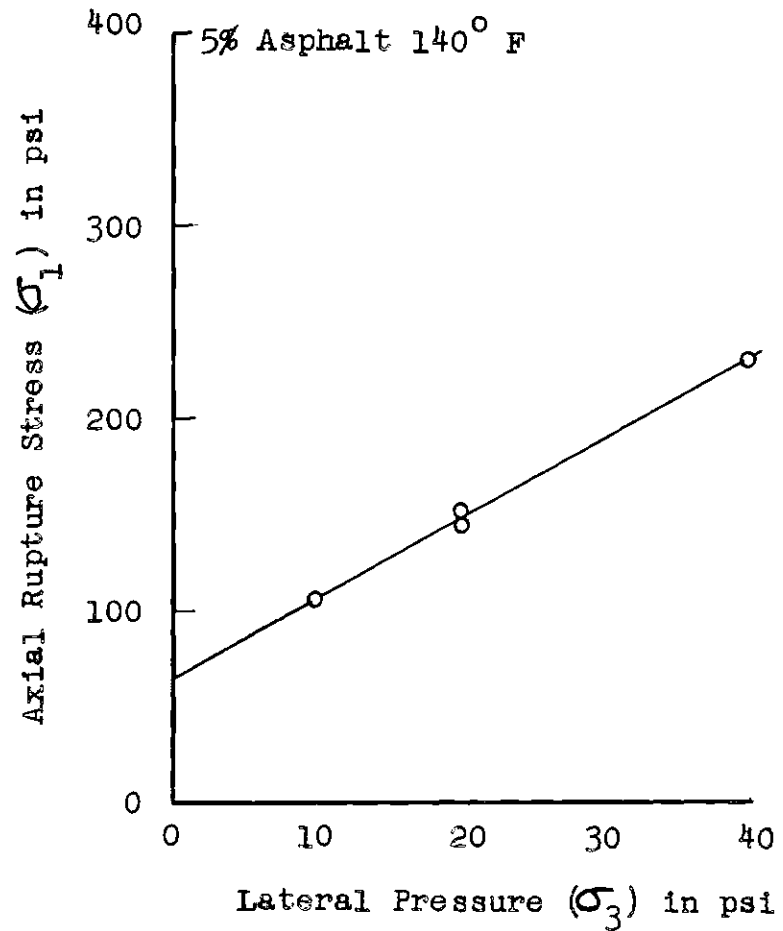


Figure 24. Axial Stress at Rupture vs. Lateral Pressure for Specimens Containing 5.0 per cent Asphalt at 140°F.

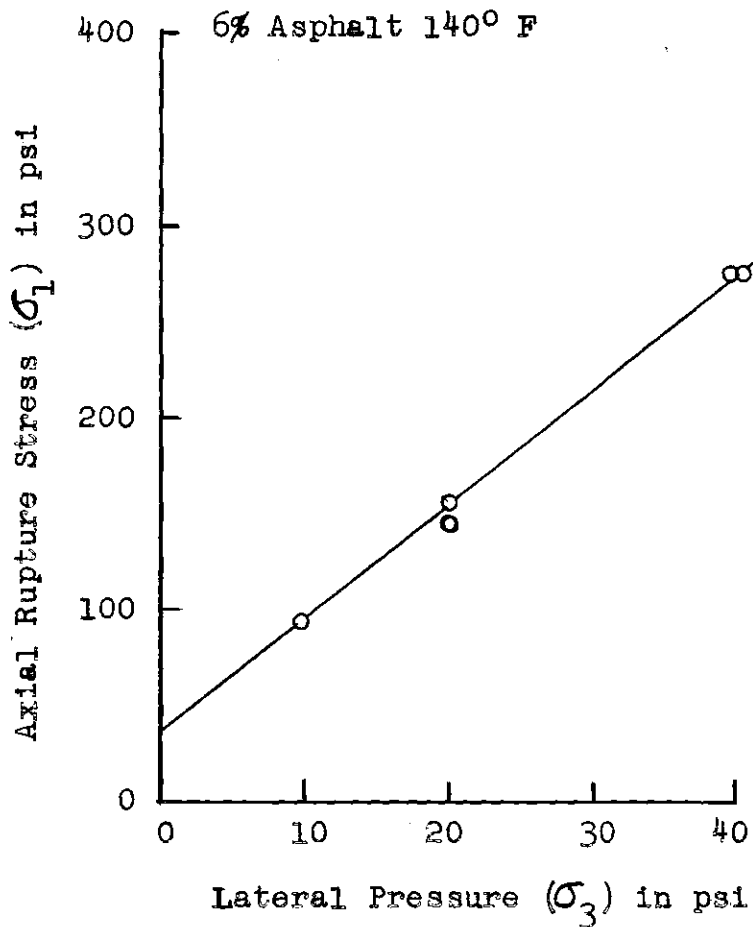


Figure 25. Axial Stress at Rupture vs. Lateral Pressure for Specimens Containing 6.0 per cent Asphalt at 140° F.

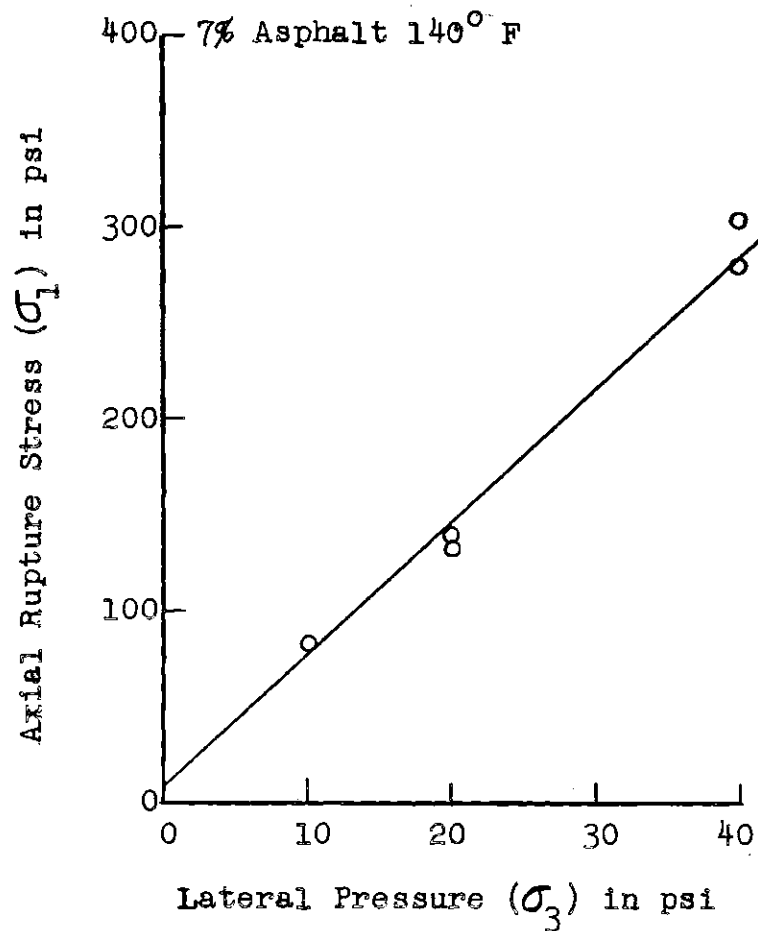


Figure 26. Axial Stress at Rupture vs. Lateral Pressure for Specimens Containing 7.0 per cent Asphalt at 140° F.

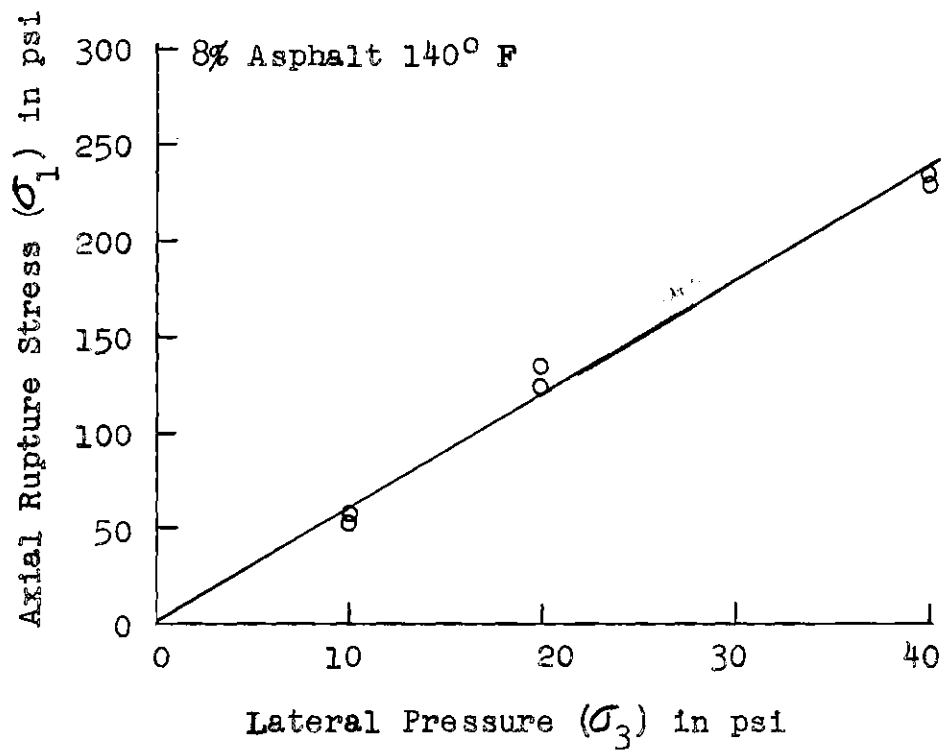


Figure 27. Axial Stress at Rupture vs. Lateral Pressure for Specimens Containing 8.0 per cent Asphalt at 140° F.

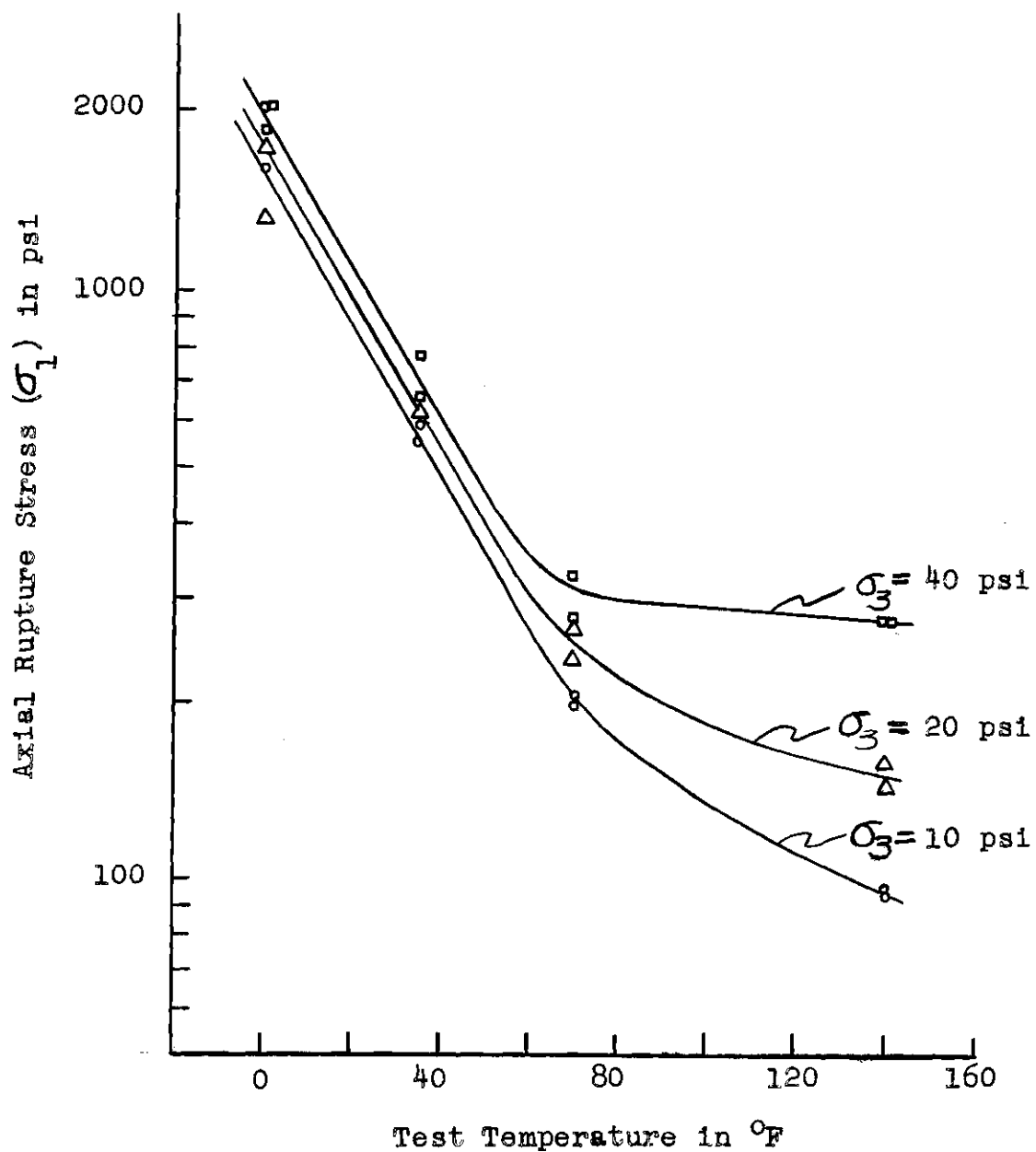


Figure 28. The Effect of Temperature on Axial Rupture Stress of Specimens Tested at Lateral Pressures of 10, 20, and 40 psi.

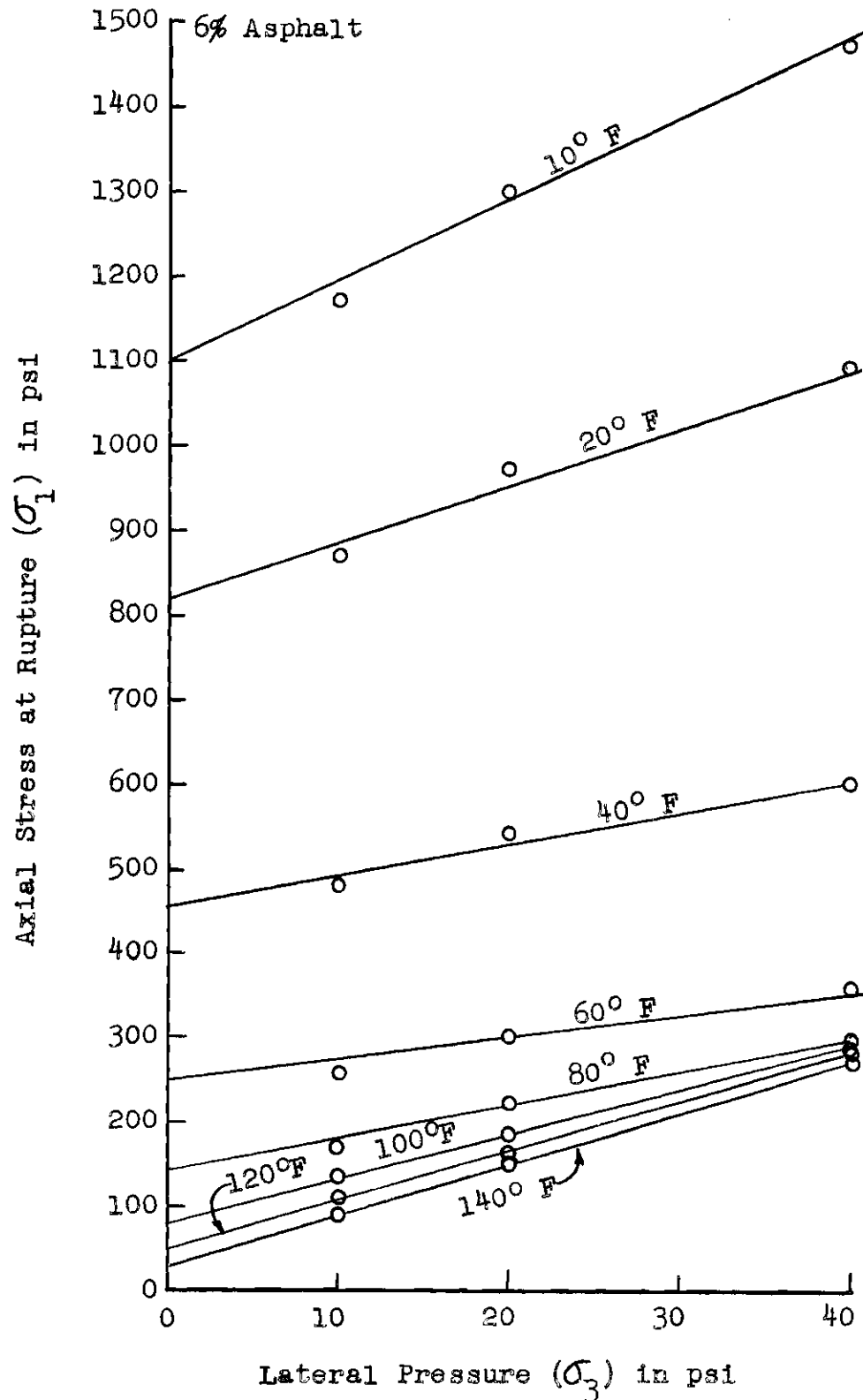


Figure 29. Axial Stress at Rupture vs. Lateral Pressure for Specimens Containing 6.0 per cent Asphalt at Test Temperatures of 0, 10, 20, 40, 60, 80, 100, 120, and 140° F.

## BIBLIOGRAPHY

## Cited References

1. Terzaghi, Karl and Peck, Ralph B., Soil Mechanics in Engineering Practice. John Wiley & Sons, New York (1948), pp. 96, 97.
2. Sowers, George B. and Sowers, George F., Introductory Soil Mechanics and Foundations. The MacMillan Co., New York (1956), p. 43.
3. Endersby, V. A., "The History and Theory of Triaxial Testing, and the Preparation of Realistic Test Specimens." Triaxial Testing of Soils and Bituminous Mixtures, American Society for Testing Materials Special Technical Publication No. 106 (1951), p. 16.
4. Ibid, pp. 16-18.
5. Hveem, F. N. and Davis, H. E., "Some Concepts Concerning Triaxial Compression Testing of Asphalt Paving Mixtures and Subgrade Materials." Triaxial Testing of Soils and Bituminous Mixtures, ASTM S.T.P. No. 106 (1951), p. 29.
6. Monismith, C. L. and Vallergera, B. A., "Relationship Between Density and Stability of Asphaltic Paving Mixtures." Proceedings, Assoc. of Asphalt Paving Technologists, Vol. 25 (1956) pp. 89-101.
7. Georgia State Highway Department, Standard Specifications for Construction of Roads and Bridges (1947), p. 188-A.
8. Mix Design for Hot-Mix Asphalt Paving, The Asphalt Institute, College Park, Maryland (1956) pp. 65-104.
9. Monismith, C. L. and Vallergera, B. A., op. cit.
10. Fundamentals of Asphalt Paving. The Ohio Oil Company, (1949) pp. 123-127.
11. Terzaghi, Karl, Theoretical Soil Mechanics, John B. Wiley & Sons, New York (1947), p. 22.

## Other References

1. Bishop, A. W. and Henkel, D. J., The Measurement of Soil Properties in the Triaxial Test. Edward Arnold (Publishers) Ltd., London (1957).

2. Hveem, F. N. and Vallerga, B. A., "Density Versus Stability." Proceedings, Assoc. of Asphalt Paving Technologists, Vol. 31 (1952).
3. Mack, Charles, "Deformation Mechanism and Bearing Strength of Bituminous Pavements." Proceedings, Highway Research Board, Vol. 33 (1954), pp. 138-166.
4. McLeod, Norman W., "Selecting the Aggregate Specific Gravity for Bituminous Paving Mixtures." Proceedings, Highway Research Board, Vol. 36 (1957), pp. 283-316.
5. Oppenlander, J. C. and Goetz, W. H., "Triaxial Testing of Bituminous Mixtures at High Confining Pressures." Proceedings, Highway Research Board, Vol. 37 (1958), pp. 201-215.
6. Nijboer, L. W., Plasticity as a Factor in the Design of Dense Bituminous Road Carpets. Elsevier Publishing Company, Inc., New York (1948).
7. Saai, R. N. J. and Labout, J. W. A., "Rheological Properties of Asphalts," Rheology Theory and Applications, Vol. II, Edited by Frederick R. Eirich. Academic Press Inc., New York (1958), pp. 388-400.
8. Vallerga, B. A., "The Triaxial Institute and the Stabilometer." Proceedings, Assoc. of Asphalt Paving Technologists, Vol. 34 (1955).
9. Van der Poel, C., "Road Asphalt." Building Materials, Ch. IX, Edited by M. Reiner and A. G. Ward. Interscience Publishers, Inc., New York (1954), pp. 391-412.